

*Exploring Simple Catalyst for Transfer Hydrogenation of Ketones and  
Photocatalytic Hydrogen Production Using Homogeneous Metal  
Complexes*

*By*

*Sara Ahmadi*

*A thesis submitted to the  
Faculty of Graduate And Postdoctoral Studies  
University of Ottawa  
In partial fulfillment of the requirements  
For the degree of  
Master of Science in Chemistry*

Department of Chemistry and Biomolecular Science  
Faculty of Science  
University of Ottawa

© Sara Ahmadi, Ottawa, Canada, 2019



uOttawa

L'Université canadienne  
Canada's university

## Abstract

Transfer hydrogenation has been recognized to be an important synthetic method in both academic and industrial research to obtain valuable products including alcohols.

Transition metal catalysts based on precious metals, such as Ru, Rh and Ir, are typically employed for this process. This thesis starts with a study on the potential of an Fe based complex carrying a PNP ligand (2,6-{Ph<sub>2</sub>PNH}<sub>2</sub>(NC<sub>5</sub>H<sub>3</sub>)) to function as an active transfer hydrogenation catalyst for the conversion of ketones to alcohols. During the analysis of the performance parameters of this potential catalyst, it was discovered that the added base, KO<sup>t</sup>Bu, was the actual catalyst. Other bases were explored as catalysts for this transformation as well as the general performance features of this simple alkali metal base.

In a separate project described in Chapter 3, the search for catalysts shifted focus to a study of the potential of a series of first row transition metal-based complexes supported by a bis(thioether)pyridine “SNS” ligand for photocatalytic hydrogen production. This initial study led to the observation that the Fe complex [Fe(κ<sup>3</sup>-2,6-(CH<sub>3</sub>SCH<sub>2</sub>)<sub>2</sub>C<sub>5</sub>H<sub>3</sub>N)Br<sub>2</sub>]<sub>2</sub> was a capable photocatalyst for H<sub>2</sub> production in combination with a photosensitizer (Ru(bpy)<sub>3</sub><sup>2+</sup>) and an electron donor (triethanolamine). Although water was initially believed to be the source of protons that were reduced to H<sub>2</sub>, analysis of control experiments pointed to the hydrogen source being the electron donor.

## Acknowledgements

First and foremost, I would like to thank my supervisor Prof. Darrin Richeson for accepting me as one of his graduate students and giving me this opportunity to learn and gain skills in a peaceful environment, I could not have gotten through my master's degree without him. I would like to thank Bulat Gabidullin for his crystallographic expertise, Yasmeen Hameed for her precious guidance, and thank all members of Richeson group for their support and the time they have spent to teach me numerous things from instrumentations to theoretical issues. The experience I have gained during these two years is priceless. Over the period of these two years I have made a lot of friends all around the chemistry department and I had the chance of having international friends and being familiarized with different cultures. Last but certainly not least, I would like to thank my uncle, Mike Ahmadi, who helped me to pursue my dream of studying in a great school in the wonderful city of Ottawa in Canada. Last but certainly not least, I would like to thank my family specifically my mother and dedicate this thesis to her as she raised me as a single mother, always supported me and motivated me to fight difficulties and resist against the storm of living alone in a foreign country.

# Table of Contents

Abstract.....	i
Acknowledgements.....	ii
Table of Contents.....	iii
List of Tables.....	iv
List of Figures.....	vii
List of Schemes.....	viii
List of Abbreviations.....	ix

## Chapter 1 “Introduction”

Introduction.....	1
1.1 Hydrogenation and Transfer Hydrogenation.....	1
1.2 Photochemical Hydrogen production.....	11
Components for a Photocatalytic Reduction Systems and Performance Parameters.....	13
Basic Mechanism of Photocatalytic Reactions.....	21
Scope and Research Content of Thesis.....	23
References.....	24

## Chapter 2 “Catalytic Transfer Hydrogenation in the Absence of a Transition Metal. Potassium*tert*-Butoxide as a Simple and Effective MPV Catalyst for Ketone Hydrogenation.”

Introduction.....	26
Results and Discussion.....	27
Investigation of the optimal reaction conditions for transfer hydrogenation of carbonyl compounds.....	27

Investigation of the substrate scope for transfer hydrogenation of carbonyl compounds using 2-PrOH as both solvent and hydrogen donor.....	37
Experimental.....	39
Proposed Mechanism.....	40
Future Work.....	42
Conclusion.....	42
References.....	43

**Chapter 3 “Photocatalytic Hydrogen Production using Earth-Abundant Metal Catalysts with Unprecedented Coordination Environments”**

Introduction.....	44
Results and Discussion.....	47
Proposed Mechanism.....	56
Experimental .....	57
References.....	62

**Chapter 4**

Conclusion.....	64
-----------------	----

**List of Tables**

Table 2.1. Experiments carried out to determine the activity of the iron complex 1 in the TH catalysis of acetophenone. All the reactions were performed under N <sub>2</sub> atmosphere in 5mL of refluxing 2-PrOH for 24h at 80°C.....	30
Table 2.2. Examining the effectiveness of different bases in a benchmark TH reaction shown in Scheme 2.2. Reactions were carried out for 24h at 80°C, in an N <sub>2</sub> atmosphere with 2.5ml 2-propanol.....	31

Table 2.3. The effect of different loadings of KO <sup>t</sup> Bu on conversion for the reaction in Scheme 2.2. Reaction time was 24h at 80°C, under N <sub>2</sub> , with 2.5ml of 2-propanol.....	32
Table 2.4. Percent Yield of 1-phenylethanol using different loading of KO <sup>t</sup> Bu, condition: 1mmol Acetophenone, Time: 2h, Temperature: 80°C, Under N <sub>2</sub> , Solvent: 2-propanol 2.5ml.....	34
Table 2.5. Percent Yield of 1-Phenylethanol for different reaction time using 1mmol acetophenone, 10 mol% KO <sup>t</sup> Bu, in 2.5ml 2-PrOH for 24h, at 80°C, under N <sub>2</sub> .....	35
Table 2.6. The effect of temperature on the percent yield of 1-Phenylethanol using 1mmol Acetophenone, 10mol% KO <sup>t</sup> Bu, under N <sub>2</sub> , with 2.5ml 2-PrOH after 15h.....	36
Table 2.7. Substrate scope of carbonyl derivatives for KO <sup>t</sup> Bu-catalyzed transfer hydrogenation using 2-PrOH as hydrogen source and solvent.....	38
Table 3.1. Photochemical H <sub>2</sub> generation from water for the series M( $\kappa^3$ -2,6-(CH <sub>3</sub> SCH <sub>2</sub> ) <sub>2</sub> C <sub>5</sub> H <sub>3</sub> N)Br <sub>2</sub> (M = Mn, Fe, Co, Ni, Cu, Zn). All reactions employed 1mmol of complex and photosensitizer, [Ru(bpy) <sub>3</sub> ](PF <sub>6</sub> ) <sub>2</sub> in 4ml of reaction solvent (DMF) with 0.2ml of added water. The electron donors, triethanolamine (TEOA), triethylamine (TEA) and 1-Benzyl-1,4-dihydronicotinamide (BNAH) were employed. Irradiation with 405 nm LED light conducted under an N <sub>2</sub> atmosphere for 24 h.....	47
Table 3.2. Photochemical H <sub>2</sub> generation using [Fe( $\kappa^3$ -2,6-(MeSCH <sub>2</sub> ) <sub>2</sub> NC <sub>5</sub> H <sub>5</sub> )Br <sub>2</sub> ] <sub>2</sub> as catalyst. All reactions were carried out with 1mmol of complex and photosensitizer, [Ru(bpy) <sub>3</sub> ](PF <sub>6</sub> ) <sub>2</sub> in 4ml of DMF with 0.2ml of added water and conducted under an N <sub>2</sub> atmosphere for 24 h. Irradiation wavelength was 405 nm. a) 1ml, b) 0.2mg 1-Benzyl-1,4-dihydronicotinamide (BNAH).....	49

Table 3.3. Photochemical H <sub>2</sub> generation from water using [Fe{κ <sup>3</sup> -2,6-(MeSCH <sub>2</sub> ) <sub>2</sub> NC <sub>5</sub> H <sub>5</sub> }Br <sub>2</sub> ] <sub>2</sub> . All reactions were carried out with 1mmol of complex and photosensitizer, [Ru(bpy) <sub>3</sub> ](PF <sub>6</sub> ) <sub>2</sub> in 4ml of reaction solvent and 1ml TEOA with 0.2ml of added water conducted under an N <sub>2</sub> atmosphere for 24 h. Irradiation wavelength was 405nm.....	49
Table 3.4. Photochemical H <sub>2</sub> generation from water using [Fe{κ <sup>3</sup> -2,6-(MeSCH <sub>2</sub> ) <sub>2</sub> NC <sub>5</sub> H <sub>5</sub> }Br <sub>2</sub> ] <sub>2</sub> . All reactions were carried out with 1mmol of complex and photosensitizer, in 4mL of DMF and 1ml TEOA as the ED with 0.2ml of added water conducted under a N <sub>2</sub> atmosphere for 24 h. Irradiation wavelength was 405nm.....	50
Table 3.5. Photochemical H <sub>2</sub> generation from water using [Fe{κ <sup>3</sup> -2,6-(MeSCH <sub>2</sub> ) <sub>2</sub> NC <sub>5</sub> H <sub>5</sub> }Br <sub>2</sub> ] <sub>2</sub> . All reactions were carried with complex and photosensitizer, in 4mL of DMF and 1ml TEOA with 0.2ml of added water conducted under an N <sub>2</sub> atmosphere for 24 h. Irradiation wavelength was 405nm.....	52
Table 3.6. Results from different time of irradiation of LED light.....	53
Table 3.7. Blank reactions. Each reaction was done under N <sub>2</sub> atmosphere for 24h with irradiation wavelength of 405nm.....	54
Table 3.8. Results from addition of different amounts of water on the photochemical H <sub>2</sub> production.....	54
Table 3.9. Results of the photochemical reaction with no water in the presence of the reactive EDs.....	55
Table 3.10. Results of the addition of different amounts of TEOA.....	56

## List of Figures

Figure 1.1. The $\eta^5$ -Cp*-rhodium complexes 1a and 1b bearing a bis(phosphine)amine ligand. (1a: X= S, 1b: X= O).....	4
Figure 1.2. Examples of bimetallic hydrogenase enzymes.....	12
Figure 1.3. The structures of some well-known electron donors used in photochemical reactions.....	15
Figure 1.4. The structure of $[\text{Ru}(\text{bpy})_3]^{2+}$ complex.....	18
Figure 1.5. Some examples of active complexes for photocatalytic hydrogen production.....	20
Figure 1.6. $[\text{Cu}(\text{dsbtmp})_2]\text{PF}_6$ Photosensitizer.....	21
Figure 2.1. Crystal structure of Complex 1.....	29
Figure 2.2. Graphical presentation of the results given in Table 2.3, showing the relation between the amount of catalyst in mol% and the yield% for 2h.....	35
Figure 2.3. Graphical presentation of the results shown in Table 2.4, showing the relation between the reaction time and the yield%.....	36
Figure 2.4. Graphical view of the data in Table 2.5, showing the relation between different temperatures and the yield% for 15h.....	37
Figure 3.1. Spectra demonstrating the quenching of the emission from the photosensitizer $\text{Ru}(\text{bpy})_3(\text{PF}_6)_2$ with various concentrations (0-3.75 mM) of TEOA. ....	51
Figure 3.2. Spectra demonstrating the quenching of the emission from the photosensitizer $\text{Ru}(\text{bpy})_3(\text{PF}_6)_2$ with various concentrations (0-0.6mM) of Fe-SNS complex.....	51
Figure 3.3. Graphical presentation of the results shown in Table 3.6, showing the relation between the productivity of the catalyst and Time.....	53

Figure 3.4. Photographs of the irradiation apparatus used for the photocatalytic experiments before and during the light irradiation.....58

Figure 3.5. Calibration curve for calculation the amount of H<sub>2</sub> in the injected aliquot.....60

### List of Schemes

Scheme 1.1. Direct hydrogenation of Acetophenone .....2

Scheme 1.2. Transfer Hydrogenation of a ketone with an alcohol as the H<sub>2</sub> source.

Common conditions: Catalyst, base, reflux, 24h.....3

Scheme 1.3. Mechanism for TH using late transition metal complexes as a catalysts.....5

Scheme 1.4. Stereoselective TH of various aromatic ketones and imines using [RuCl( $\eta^6$ -arene) (N-arylsulfonyl DPEN)..... 6

Scheme 1.5. The “outer- sphere” transfer hydrogenation mechanism. D: The metal hydride transition state in “inner- sphere” mechanism.....8

Scheme 1.6. MPV reduction reaction.....9

Scheme 1.7. ATH of polar bonds using Iron-based catalysts.....10

Scheme 1.8. The proposed reactivity of the TEOA (ED) during the photocatalytic reaction.....15

Scheme 1.9. Reductive quenching and oxidative quenching diagram.....17

Scheme 2.1. The divalent Fe complex with 2,6-{Ph<sub>2</sub>PNH}<sub>2</sub>(NC<sub>5</sub>H<sub>3</sub>). Complex 1.....28

Scheme 2.2. Benchmark reaction used in this chapter. Reagent: Acetophenone, Hydrogen donor/Solvent: 2-PrOH, Base: KO<sup>t</sup>Bu, 24h, 80°C, Under N<sub>2</sub>.....29

Scheme 2.3. Proposed mechanism for transfer hydrogenation of a ketone.....41

Scheme 3.1. Summary of metal bis(thioether) pyridyl complexes used in this study.....45

Scheme 3.2. Degradation of TEOA.....56

Scheme 3.3. Proposed mechanism of catalytic cycle.....58

**List of Abbreviations**

ACN	Acetonitrile
ATH	Asymmetric Transfer Hydrogenation
BNAH	1-benzyl-1,4 dihydronicotinamide
Cat	Catalyst
DEE	Diethylether
DMT	N,N-dimethyl-p-toluidine
DMA	Dimethyl acetamide
DMF	N,N-dimethyl formamide
DPEN	1,2-diphenylethylene-1,2-diamine
ED	Electron Donor
H <sub>2</sub> A	Ascorbic Acid
MPV	Meerwein-Pondorff-Verley
NaA	Sodium Ascorbate
PS	Photosensitizer
S	Solvent
TH	Transfer Hydrogenation
TM	Transition Metal
TON	Turn Over Number
TOF	Turn Over Frequency
TEA or (NEt <sub>3</sub> )	Triethylamine
TEOA	Triethanolamine

## **Chapter 1**

### **1.Introduction**

Dihydrogen, H<sub>2</sub>, is the most abundant and simplest molecule in universe. In addition, H<sub>2</sub> is arguably among the most important and certainly one of the most interesting molecules.

The fundamental description of this species forms the basis to introduce the concepts of the molecular bond. In the chemical industry, dihydrogen is used in large quantities to produce ammonia and in a vast array of hydrogenation processes. Furthermore, H<sub>2</sub> is a promising energy carrier that has been envisioned to be a “green” fuel for the future which could be used in fuel cells and even modified internal combustion engines.

This thesis is focused on trying to explore some of these aspects of hydrogen. When this project began it was to discover and explore the transfer hydrogenation reaction, an aspect of hydrogen reactivity, and in section 1.1 a brief background of this important reaction is provided. Another interesting aspect about molecular hydrogen is its production. The second part of this thesis focuses on the discovery of new molecular catalysts for the photocatalytic generation of H<sub>2</sub>. A general overview of the literature background and concepts of this area of investigation is presented in section 1.2.

#### **1.1 Hydrogenation and Transfer Hydrogenation**

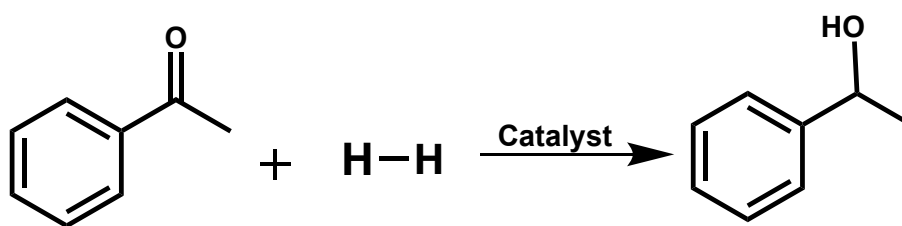
Hydrogenation is the addition of hydrogen atoms to a molecule and is one of the most fundamental and practically important of all chemical transformations. In organic synthesis, hydrogenation is commonly associated with the addition of two hydrogen atoms to a multiple bond such as the C=O or C=C bond of a molecule. Industrial

applications of hydrogenation span from the petrochemical industry to fine chemicals and pharmaceuticals synthesis.

Direct hydrogenation can be carried out using H<sub>2</sub> gas and a catalyst (Scheme 1.1). This process typically uses greater than 1 atmosphere of hydrogen. The hydrogen is generally obtained from natural gas at high temperatures in the steam reforming process (equation 1).



An alternative method of hydrogenation, called transfer hydrogenation (TH), uses a donor molecule rather than molecular H<sub>2</sub> as the hydrogen source. Typical donors are formic acid and isopropanol. These species undergo a dehydrogenation reaction and yield CO<sub>2</sub> and acetone, respectively. The hydrogen that is released by these donors is added to an unsaturated reactant. Again, catalysts are used to facilitate the transfer of H<sub>2</sub> between the two compounds. (Scheme 1.2)

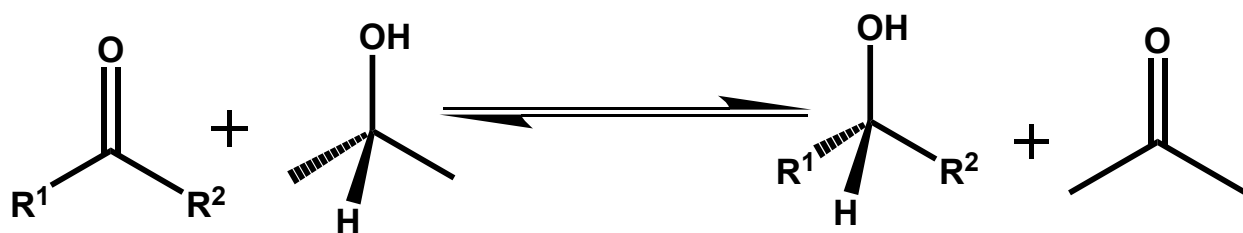


**Scheme 1.1.** Direct hydrogenation of Acetophenone

The discovery of hydrogen transfer goes back more than a century. In 1903, Knoevenagel first demonstrated that palladium black gradually promoted the disproportionation of dimethyl 1,4-dihydroterephthalate to dimethyl terephthalate and *cis*-hexahydroterephthalate where the hydrogen transfer was achieved between identical donor and acceptor units.<sup>1</sup>

Since this initial observation, transfer hydrogenation has continued to evolve and TH reactions can be categorised into three types: (i) hydrogen migration taking place within one molecule; (ii) hydrogen disproportionation, involving transfer between identical donor and acceptor units; and (iii) TH-dehydrogenation, occurring between unlike donor and acceptor units. This thesis will be focused on the last type.

Transfer Hydrogenation is a suitable and powerful method for hydrogenation of various compounds and has become the center of research in hydrogenation studies.<sup>2</sup> (Scheme 1.2)



**Scheme 1.2.** Transfer Hydrogenation of a ketone with an alcohol as the H<sub>2</sub> source  
Common conditions: Catalyst, base, reflux, 24h

There are several key reasons that transfer hydrogenation is particularly attractive. First, it does not require the use of hazardous pressurized H<sub>2</sub> gas. Second, hydrogen donors are readily available, inexpensive, and easy to handle. A third attractive feature is that the side products coming from the dehydrogenated H<sub>2</sub> source species are recyclable. Finally, the catalysts that can be used in TH reactions usually are accessible, and not sensitive.<sup>3</sup> The design and exploration of molecular catalysts for TH began with the observations that some complexes of Ir, Ru and Rh were active in this role. As a result, complexes of these precious metal centers were targeted in an effort to develop new and active catalysts. Such complexes bearing N, P, O, S, C based ligands with various forms such as metal-N-heterocyclic carbenes, half sandwich, multidentate metal complexes, and

their combinations have been developed.<sup>3</sup> The pioneering work reported by Henbest, Mitchell, and co-workers in the 1960s<sup>4</sup> showed the catalytic hydrogenation of cyclohexanones and  $\alpha,\beta$ -unsaturated ketones to alcohols with isopropanol with an iridium hydride complex.<sup>3</sup>

These results were followed in the 1970s, and Sasson and Blum's work on  $[\text{RuCl}_2(\text{PPh}_3)_3]$ , showed that the  $[\text{RuCl}_2(\text{PPh}_3)_3]$  complex was productive in biphasic TH of acetophenone with isopropanol at high temperature.<sup>5</sup> Later in the 1990s, Chowdhury and Bäckvall showed that by adding a catalytic amount of NaOH, this reaction was accelerated by  $10^3$ – $10^4$  times.<sup>6</sup> In rhodium-catalyzed transfer hydrogenation, the half-sandwich rhodium complexes have demonstrated successful catalytic behavior. The  $\eta^5$ -Cp\*-rhodium complexes **1a** and **1b** bearing a bis(phosphine)amine ligand (Figure 1.1), gave 94-99% conversion of the transfer hydrogenation of substituted acetophenones in isopropanol at reflux.<sup>7</sup>

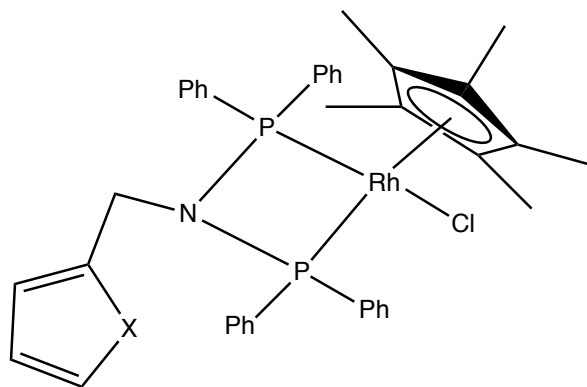
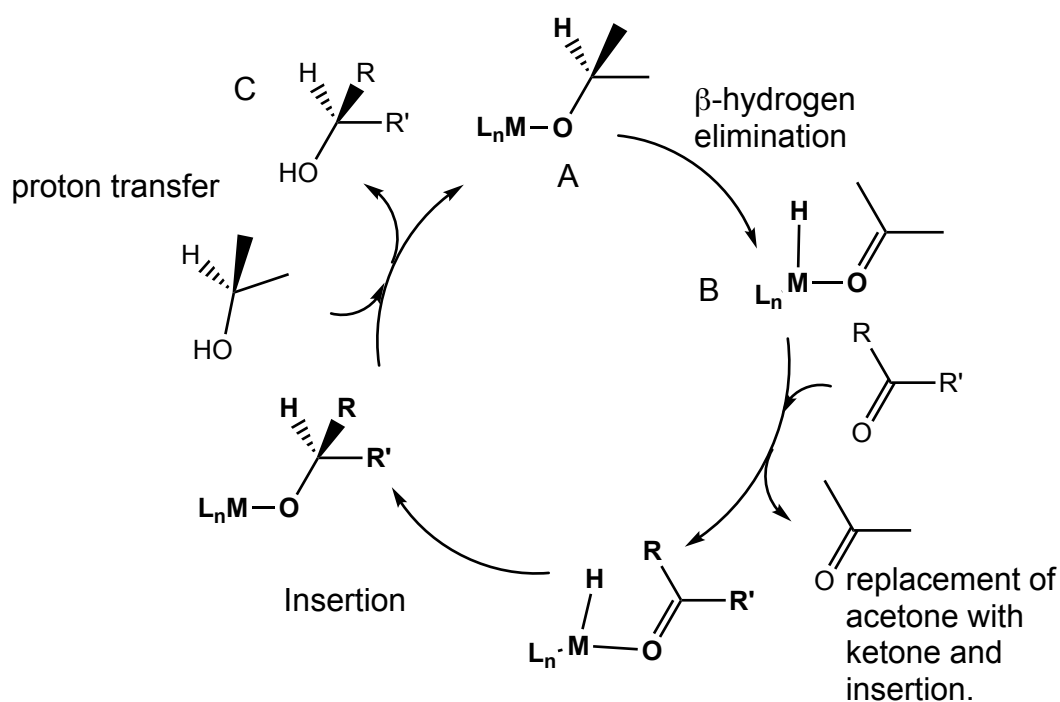


**Figure 1.1.** The  $\eta^5$ -Cp\*-rhodium complexes **1a** and **1b** bearing a bis(phosphine)amine ligand. (**1a**: X= S, **1b**: X= O)

Late transition metal complexes when coupled with a base (e.g. NaOH, KOH, or  $\text{K}_2\text{CO}_3$ ) are catalysts for transfer hydrogenation of ketones using 2-propanol as the hydrogen source. In addition to isopropanol, formic acid has been used in the conversion of carbonyl compounds to alcohols. The role of the base is important for the success of these

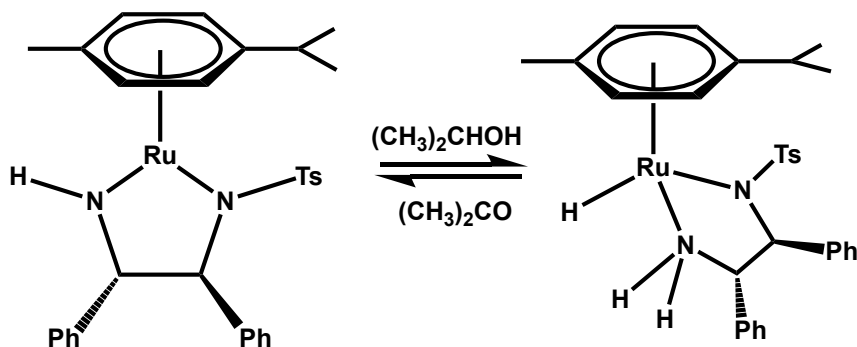
catalysts and functions by promoting the deprotonation of the isopropanol to produce the isopropoxide anion which undergoes a substitution reaction with the transition metal. The currently accepted mechanism for transition metal catalyzed TH is outlined in Scheme 1.3. After formation of the metal isopropoxide complex **A**, a  $\beta$ -hydrogen elimination forms the M-H complex **B**. Next there is the replacement of acetone with substrate ketone and insertion. Finally, through proton transfer the free alcohol product **C** is released and the starting isopropoxide complex is regenerated. In this mechanism the transformation of the substrate occurs within the coordination sphere of the metal and thus this mechanism has been called the “inner sphere” mechanism in order to differentiate it from the ligand assisted (outer-sphere) mechanism described below.



**Scheme 1.3.** “Inner-sphere” mechanism for TH using late transition metals as a catalyst.

The “inner-sphere” mechanism is captured by common elementary steps of organometallic transformations. While working on methods to produce catalysts capable of asymmetric transfer hydrogenation, Noyori and co-workers developed a number of Ru(II) complexes with chiral ligands. Particular success was achieved with complexes containing an N-tosylated ethylenediamine ligand.  $[\text{RuCl}(\eta^6\text{-arene})(\text{N-arylsulfonyl-DPEN})]$  (DPEN = 1,2-diphenylethylene-1,2-diamine) (Scheme 1.4) was used as catalyst for stereoselective TH of various aromatic ketones and imines.<sup>8</sup>

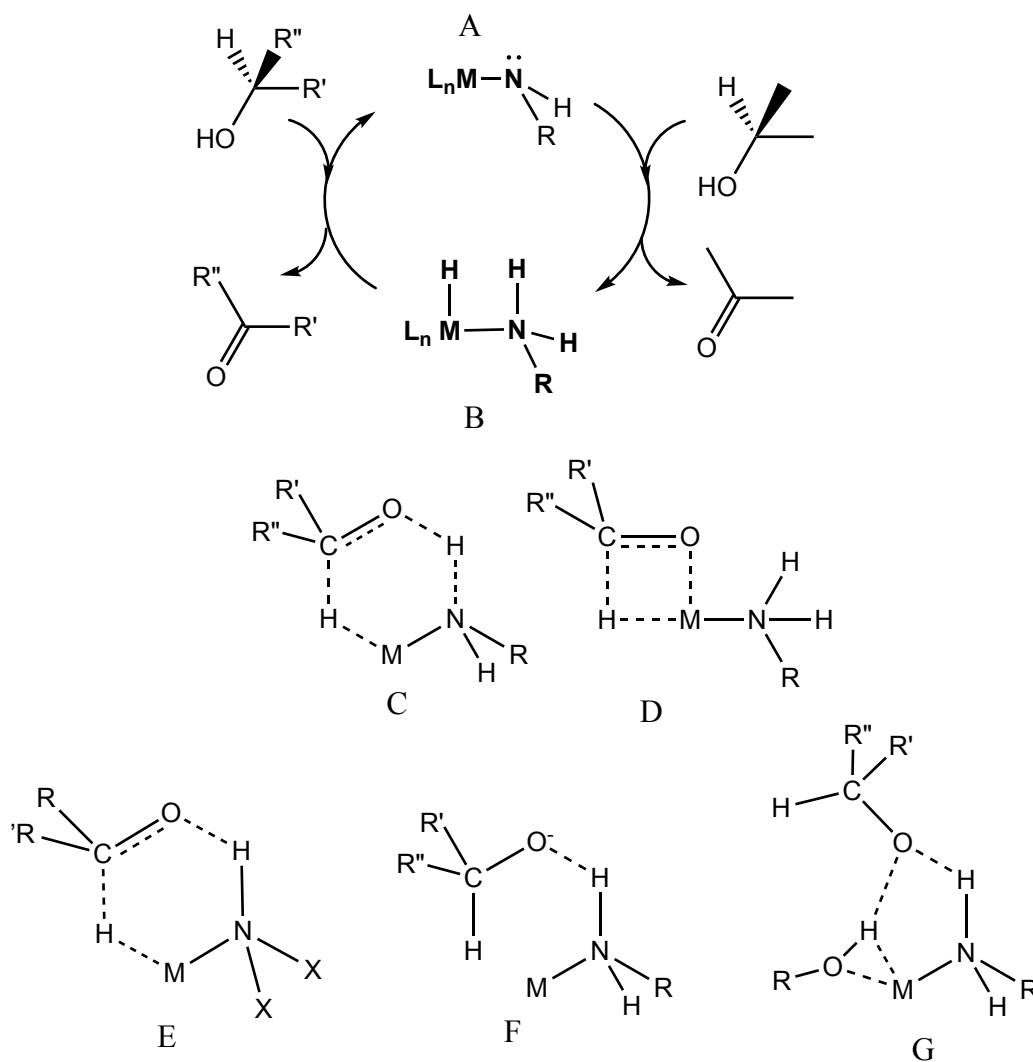
These Ru complexes achieved highly efficient asymmetric transfer hydrogenation of ketones and imines and the presence of an NH moiety in the ligands is crucially important. Further investigations led to a mechanism involving metal-ligand bifunctional catalysis where the NH linkage stabilizes the transition state through formation of a hydrogen bond with a ligand N center. The resulting six-membered cyclic transition structure is schematically represented in Scheme 1.5.



**Scheme 1.4.** Stereoselective TH of various aromatic ketones and imines using  $[\text{RuCl}(\eta^6\text{-arene})(\text{N-arylsulfonyl-DPEN})]$

This alternative transfer hydrogenation mechanism takes place by a novel metal-ligand bifunctional mechanism outlined in Scheme 1.5. This mechanism has been termed an “outer-sphere” mechanism to contrast with the “inner-sphere” process. The process begins with a 16-electron species Ru amide (**A**) which is transformed to an 18e MH

complex (**B**) by dehydrogenation of 2-propanol via a six-membered cyclic transition state (**C**). Coupled with the generation of the MH linkage is formation of an NH unit in the ligand attached to the metal center. The product ketone (e.g. acetone) is released in this step. The hydrogen addition to the C=O function employs this metal hydride and proceeds through a six-membered transition state similar to that of the dehydrogenation step (**C**) in which the NH function participates. This contrasts with the conventional insertion of the C=O bond into the M-H linkage shown in (Scheme 1.3). This nonclassical mechanism is characterized by the direct participation of the metal and the surrounding ligand in both dehydrogenation bond breaking and hydrogenation bond forming steps. Neither a carbonyl oxygen atom nor an alcoholic oxygen interacts with the metallic center throughout the hydrogen transfer processes. Because of this feature, the carbonyl reduction has been characterized as an “outer-sphere” mechanism. The nonclassical metal-ligand bifunctional mechanism provides a pathway for hydrogenation of unsaturated bonds that does not require ligation to the metallic center and in which both hydride and proton are simultaneously delivered to the substrate from MH and NH groups. When the coordinatively saturated metal hydride species provides a chiral surface the ketone enantiofaces can be discriminated. This contrasts with most other asymmetric hydrogenations where enantioface discrimination arises from an interaction between the metal and substrate. The stereoselectivity of the transition state structure is determined by steric and electronic factors that involve the secondary interaction between nonreacting sites. This interaction is important in generating the kinetic bias needed for asymmetric induction.

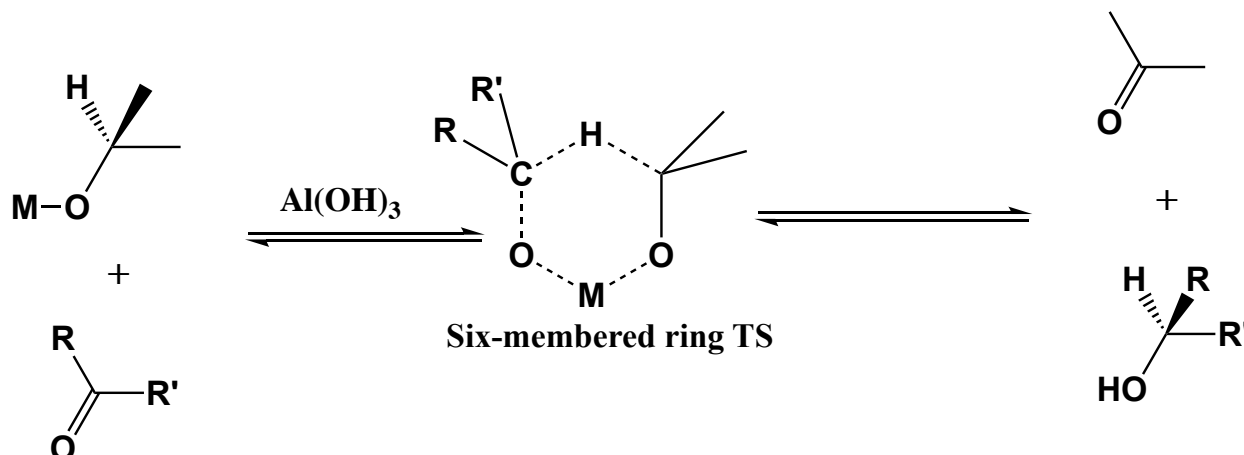


**Scheme 1.5.** The “outer- sphere” transfer hydrogenation mechanism.  
 D: The metal hydride transition state in “inner- sphere” mechanism.

Although this mechanism has been generally accepted for the last 15 years recently, Dub and coworkers have brought this mechanism into question. They have proposed an alternative which replaces the concerted transfer of hydrogen with a stepwise transfer of hydrogen atoms, both originating from the MH group with the NH bond remaining intact (Scheme 1.5, E-G) but stabilizing the intermediates/transition states of the reaction.<sup>9</sup>

In addition to the transition metal catalyzed transfer hydrogenation processes that have been described, the Meerwein-Ponndorf-Verley (MPV) reaction has been well-known since 1925 and is actually the first TH reaction to use carbonyl compounds. These reactions originally employed aluminum alkoxide ( $\text{Al(OR)}_3$ ) catalysis. In the original MPV reaction, an aluminum alkoxide was used to catalyze the reduction of an aldehyde or ketone to the corresponding alcohol in the presence of an alcohol as the hydrogen donor. Generally these reactions required greater than stoichiometric amounts of  $\text{Al(OR)}_3$ . More recently success has been achieved with catalytic amounts of Al complexes.<sup>1,10</sup>

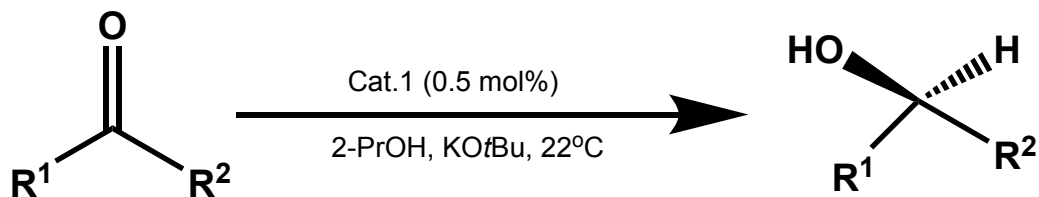
In the homogeneous MPV reduction, a direct TH through the formation of a cyclic six-membered transition state in which both the reducing alcohol and the carbonyl are coordinated to the same metal center was proposed to take place (Scheme 1.6).

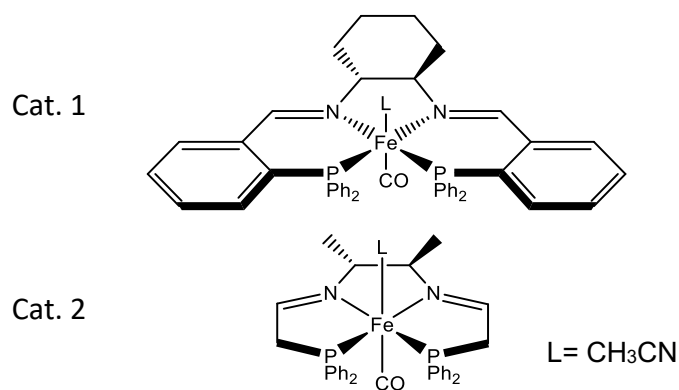


**Scheme 1.6.** MPV reduction reaction.

From a historical perspective, the Al catalyzed MPV reaction is the older process and these reactions began to take a lower profile as research efforts in transition metal catalyzed reactions took on a more active role beginning in the 1960's. The likely reason for this shift in focus is the ability to tune the ligand environment of transition metal complexes allowing for controlling reaction selectivity and for the design and development

of asymmetric TH (ATH) reactions. The ability to change the metal and ligand identity made these research efforts appealing and productive and allowed expansion of the scope of unsaturated starting materials to include, for example, imines. More recently, there has been a desire to move away from complexes of Ru, Ir, and Rh, due to the expense and rarity of these metals. The focus has moved to the exploitation of other late and particularly first row transition metals such as Fe<sup>11</sup>, Co<sup>12</sup>, and Ni<sup>13</sup> is an active and productive field. Particular emphasis has been on the more earth abundant transition metals and Fe complexes are fascinating candidates for a “greener” alternative to precious metals. Fe is the most abundant TM on earth’s crust, inexpensive, environmentally benign, and has a very low toxicity. A pioneering breakthrough in the development of iron-catalyzed ATH reactions was reported by Morris and co-workers<sup>14</sup> who designed the iron(II) complexes (Cat1 and Cat2) containing tetradentate diiminodiphosphine “PNNP” ligands inspired by the high activity and enantioselectivity of Ru–PNNP complexes in TH and hydrogenation using H<sub>2</sub>.<sup>15</sup> The new Fe complex [trans-Fe(CO)(NCMe)(CyP<sub>2</sub>N<sub>2</sub>)] [BF<sub>4</sub>]<sub>2</sub> (Cat1) displayed a good activity in ATH of ketones, aldehydes, and imines under very mild conditions using 2-PrOH as the hydrogen donor, affording turnover frequencies of up to 995 h<sup>-1</sup> (Scheme 1.7).<sup>14</sup>





**Scheme 1.7.** ATH of polar bonds using Iron-based catalysts

Bases play an important role in these reactions as they act as a co-catalyst. Examples of bases that have been employed in TH are Et<sub>3</sub>N, KOH, NaOH, Na<sub>2</sub>CO<sub>3</sub>, 2-PrOK, 2-PrONa, KO<sup>t</sup>Bu, NaO<sup>t</sup>Bu, K<sub>3</sub>PO<sub>4</sub>, Cs<sub>2</sub>CO<sub>3</sub> and NaOMe. The pK<sub>a</sub> value and the cationic or anionic nature of the base influence the catalytic efficiencies of transition-metal catalysts.<sup>3</sup> As one of the most important reactions for the synthesis of many bulk and fine chemical products, the development of benign catalytic reactions which follow the principles of green chemistry for TH has become a significant concern and activity for many academic and industrial researchers.<sup>16</sup>

## 1.2 Photochemical Hydrogen production

The global dependence on fossil fuels as a source of energy and as raw materials for industrial products presents increasing challenges to our society, environment and economy. Two obvious detrimental features derive from the fact that fuels are finite, and their combustion to supply the major source of energy in industry has caused a drastic rise of atmospheric CO<sub>2</sub> levels.<sup>17</sup> Worldwide energy demand continues to increase and fossil fuel combustion continues to provide the primary source to meet this demand.<sup>18</sup> Alternative and renewable sources such as wind, water, and solar power are rapidly

growing to fill some of this demand, but their discontinuity makes energy storage an on-going challenge and these sources are not efficient to fulfill transport requirements. In order to provide sustainable resources for fuels and commodity production 'Solar fuels' attract continued interest.<sup>19</sup> These energy sources rely on the direct conversion of sunlight into chemical bonds which serve as a fuel. This process requires the help of an artificial photocatalyst<sup>20</sup> and is inspired by the first step of natural photosynthesis where water is photocatalytically split into oxygen and hydrogen. The H<sub>2</sub> is derived from protons and electrons extracted from H<sub>2</sub>O. The H<sub>2</sub> from this process is used in nature to react with CO<sub>2</sub> to form organic compounds.

Hydrogenases (H<sub>2</sub>ase) are a group of natural enzymes (found in 99% of organisms, mostly bacteria) that can catalyze the reversible redox transformation of hydrogen with protons. There are three types of hydrogenases. There is a mononuclear Fe species and two bimetallic types that have either FeFe or FeNi cores. The bimetallic enzymes are capable of both oxidation of H<sub>2</sub> and reduction of H<sup>+</sup>. The names of these enzyme reflect the composition of its bimetallic active sites: the [FeNi]-H<sub>2</sub>ase displays an Fe-Ni core and the [FeFe]-H<sub>2</sub>ase utilizes two iron centers (Figure 1.2). [FeFe]-H<sub>2</sub>ase carries biologically unusual organometallic CO and CN<sup>-</sup> on Fe atoms, with thiolates as the remaining donors in both terminal and bridging ( $\mu$ ) positions.<sup>19</sup> The [FeFe]-H<sub>2</sub>ase is a type of metalloenzyme being famous for catalytic H<sub>2</sub> generation, reversibly interconverting two electrons and two protons into molecular hydrogen.

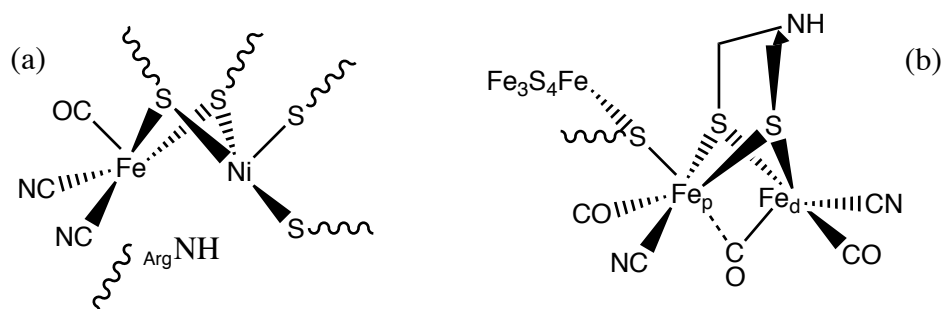


**Figure 1.2.** Examples of bimetallic hydrogenase enzymes.

Detailed mechanistic characterization of H<sub>2</sub>ases is still under investigation, but it has been verified that in all cases they operate through reversible heterolytic dissociation of the H–H bond into a metal-hydride and a proton. The hydride occupies a terminal position on the “distal” iron (Fe<sub>d</sub>) in [FeFe]-H<sub>2</sub>ases, where azadithiolate cofactor, HN(CH<sub>2</sub>S)<sub>2</sub><sup>2-</sup>, provides a neighboring amine group that acts as the proton acceptor.<sup>21</sup> It should not be neglected that a proximal proton acceptor site plays a crucial role in the mechanism of H<sub>2</sub>ases and is a feature applicable to the activity of molecular complexes.<sup>22</sup>

Hydrogenase enzymes in nature produce hydrogen with a very high turnover number and excellent selectivity but, they are very sensitive to their functional conditions such as pH, and temperature. In addition, it is very expensive to isolate them for large-scale productions. Therefore, artificial photocatalysts which display a wider tolerance to experimental conditions are a targeted field of research and have yielded some interesting preliminary results. Using the ideas outlined above, the production of artificial photocatalysts have become a center of research recently. Several complexes based on transition metals such as Fe<sup>23</sup>, Ni<sup>24</sup>, Cu<sup>25</sup> have been characterized and investigated. These catalysts usually carry one (or more) 3d transition metal center in their active sites and they cycle between different oxidation states in order to promote the addition or

extraction of electrons and protons to or from a relevant substrate by providing a binding site where this transformation can be carefully controlled.

Before getting into details of the complexes and their photocatalytic behavior there are some definitions that are necessary to understand the context of these results. Generally, the ability of metal complexes and dyes involving a single-electron-transfer processes with organic substrates following photoexcitation with visible light can be defined as photochemistry. Like in any other chemical reaction, this approach has some required components in order to take place.

### **Components for a Photocatalytic Reduction Systems and Performance Parameters**

A photocatalytic system requires some key components which include the electron donor (ED), the photosensitizer (PS), the catalyst (Cat), and the solvent (S). Each of these components that play key and interactive roles in the photocatalysis will be explained briefly below. The productivity of this system is defined by some parameters such as TON (Turn Over Number) and TOF (Turn Over Frequency).

#### **Electron Donor (ED)**

This component provides the electrons needed for the reduction reaction (i.e.  $H^+$  to  $H_2$ ). These electrons are generally transferred to the catalyst using the photosensitizer as an intermediary. The details of this process will be presented with the description of the role of the photosensitizer (PS). Many different electron donors can be used in the photocatalytic system, but there are some points that must be considered when it comes to pick the most convenient one. For example, the stability of the oxidized electron donor

(ED<sup>+</sup>) is one of the important points that should be considered because it has a large effect on the overall efficiency of the photocatalytic system due to the potential of back-electron transfer that can happen from the reduced excited state of the photosensitizer (PS<sup>\*</sup>) to the oxidized electron donor (ED<sup>+</sup>). Another key point of consideration is the reactivity of the oxidized donor and by-products. These species are always present in the reacting system and can interact with the intermediates in the photocatalytic process.

There are some commonly used electron donors in the known photocatalytic systems of H<sub>2</sub> production. These include triethanolamine (TEOA), triethylamine (TEA), 1-benzyl-1,4-dihydronicotinamide (BNAH), ascorbic acid (H<sub>2</sub>A), sodium ascorbate (NaA), and *N,N*-dimethyl-*p*-toluidine (DMT). The structures of these compounds are presented in Figure 1.3.

TEOA is perhaps the most common ED and a proposed oxidation pathway is shown as an example in Scheme 1.8. Importantly, the decomposition of the oxidized product involves both generation of protons and formation of species that can function as additional electron donating (reduction) components.

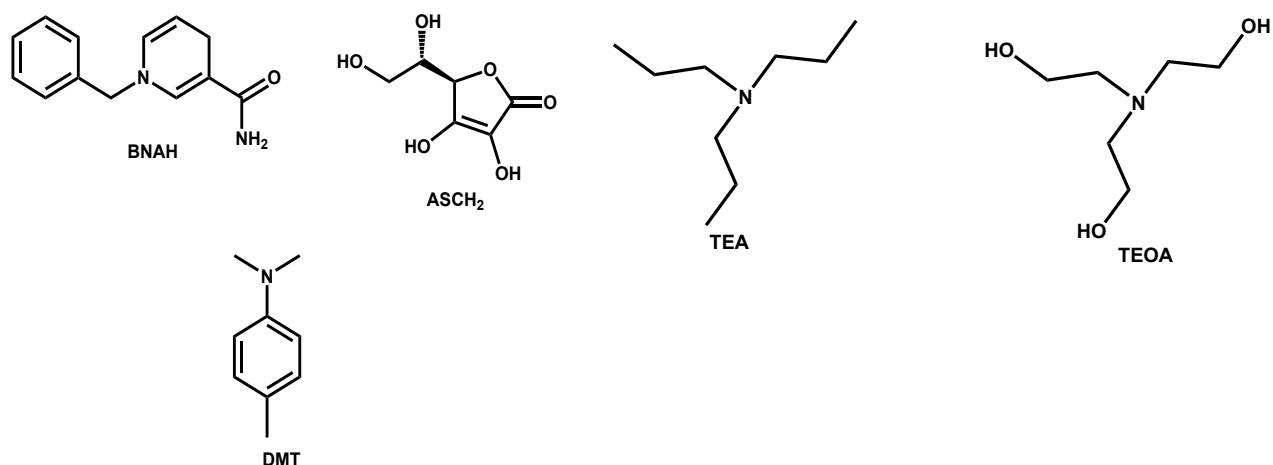
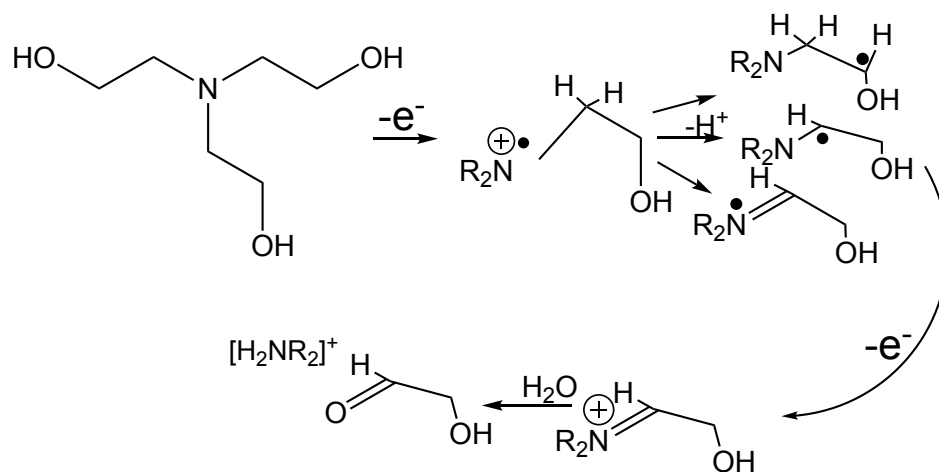


**Figure 1.3.** The structures of some well-known electron donors used in photochemical reaction.



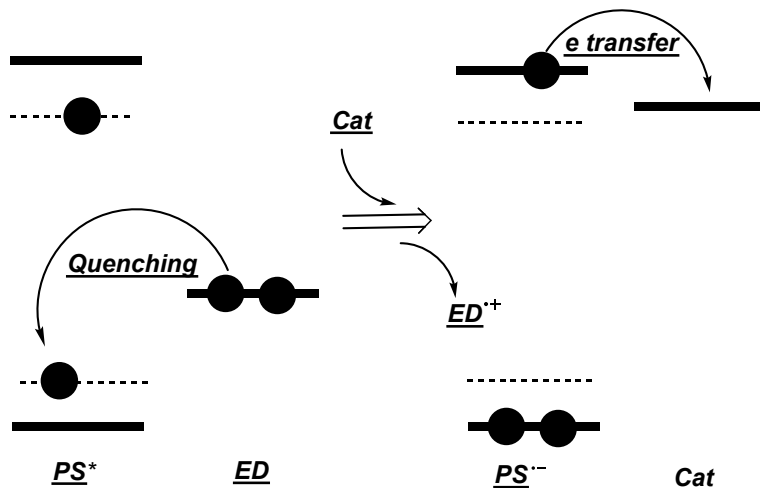
**Scheme 1.8.** The proposed reactivity of the TEOA (ED) during the photocatalytic reaction.

### Photosensitizer (PS)

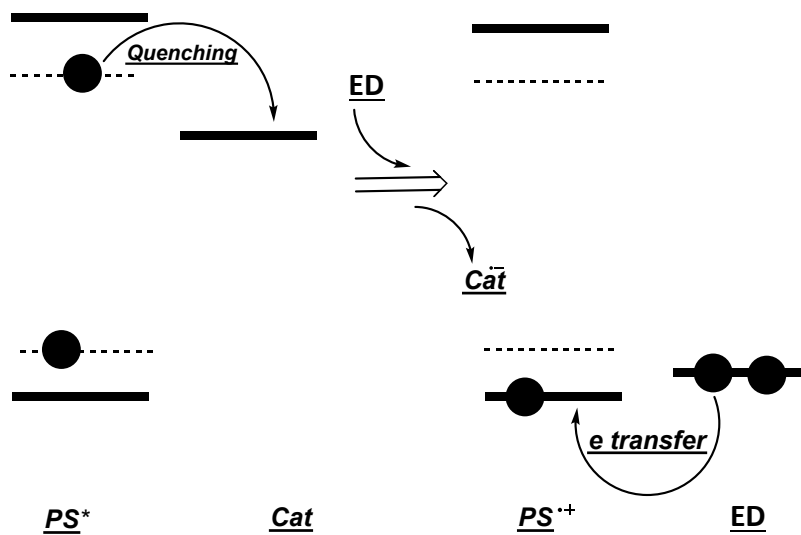
In a simple sense, the photosensitizer (PS) is a molecule that is capable of absorbing the incident light to generate an excited state species  $PS^*$  and the energy of this species is used to produce the chemical transformation. However, it is in the energy transfer where the role of the PS in transferring electrons for this photoredox reaction is slightly more complex. This electron transfer process is possible through two routes. One of these paths involves reductive quenching of the  $PS^*$  to produce  $PS^-$  and the other is the oxidative quenching of the  $PS^*$  to produce  $PS^+$ . Reductive quenching is when the excited state photosensitizer,  $PS^*$ , is reduced by the electrons coming from the ED to yield a reduced compound  $PS^-$ . The electron is then transferred from anion  $PS^-$  to the catalyst. This approach is the most commonly encountered process with photocatalytic  $H_2$  production. On the other hand, the excited state of the photosensitizer ( $PS^*$ ) can undergo oxidative quenching by reaction with the catalyst (Cat) to form a reduced catalyst ( $Cat^-$ ) and an oxidized photosensitizer,  $PS^+$ .  $PS^+$  can then be reduced by the ED to reform  $PS$ .<sup>26</sup>

Both reductive quenching and oxidative quenching processes are represented by energy diagrams in Scheme 1.9.

**Reductive Quenching**



**Oxidative Quenching**



**Scheme 1.9.** Reductive quenching and oxidative quenching diagrams

Key features that make a good photosensitizer include:

1. the ability to absorb light at longer wavelengths than the other components such as catalyst and electron donor (600-850 nm).
2. Long lasting reactive excited state
3. High stability of the one electron reduced species
4. Strong oxidation power of excited state

One of the most commonly used photosensitizers is the tris(2,2'-bipyridine) ruthenium (II) complex represented in Figure 1.4. This complex is of great interest due to its unique combination of the redox properties, its chemical stability, the excited state reactivity, and excited state lifetime.<sup>27</sup>

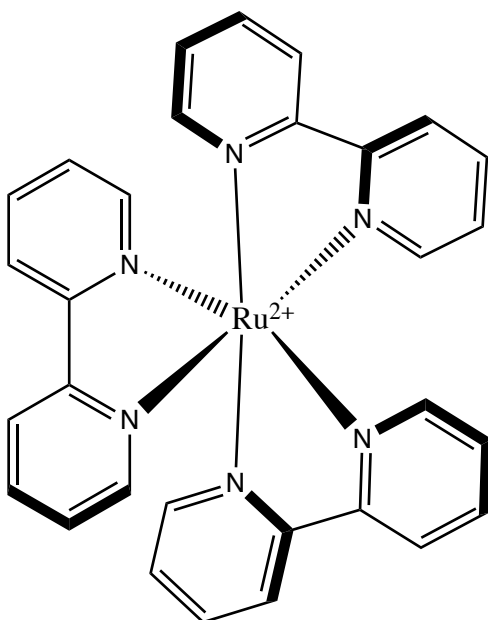


**Figure 1.4.** The structure of  $[\text{Ru}(\text{bpy})_3]^{2+}$  complex

### **Catalyst (Cat)**

The ED and PS form the light absorbing and electron transfer sources for the photocatalysis and the catalyst (Cat) forms the core reaction site component of the

photocatalytic system. There are a variety of known catalysts that in conjunction with electrons from the photosensitizer can catalytically reduce a hydrogen source. Inspiration in the design of catalysts can come from nature.

Some of the key features that a catalyst should possess are:

1. Ability to transfer between different oxidation states (redox active),
2. Ability to react with a proton,
3. Being nonphotoactive in the presence of a PS,
4. Ability to quench the PS\*,
5. High Solubility in various types of (water, organic) solvents,
6. Stable enough to go through the catalytic cycle,
7. Inexpensive and readily available, and
8. Exhibit low toxicity of both the ligand and metal center.

Figure 1.5 represents some examples of first-row transition metal catalysts that have been documented to reduce a proton source in order to produce H<sub>2</sub>.

### **The Turnover Number (TON) and Turnover-Frequency (TOF)**

The turnover number is used to describe the productivity of the catalyst. The turnover number is defined as the molar ratio of reduction products to the catalyst, as defined in equation (2).

$$TON = \frac{[Produced H_2]}{[catalyst]} \quad (2)$$

The TON is an important parameter because it is a fundamental feature of any catalyst and it indicates the stability of the catalyst.

A related parameter that is commonly used to describe the activity of the catalyst is the turnover frequency (TOF). This is given by equation (3).

$$TOF = \frac{TON}{Time} \quad (3)$$

TOF is the catalyzed reaction rate per catalyst molecule.

In order to briefly outline the interplay of the photocatalytic system components, some details for the general picture of the operating conditions and performance parameters of the photocatalyst complex  $\text{Co}(\text{dmgH})_2(\text{py})\text{Cl}$  (Figure 1.5.b) will be discussed. A typical experiment is carried out in 1:1 acetonitrile:H<sub>2</sub>O solution using DMT as the ED. The reaction has been examined using two different photosensitizers,  $\text{Ru}(\text{bpy})_3^{2+}$  (Figure 1.4) and a copper-based PS,  $[\text{Cu}(\text{dsbtmp})_2]\text{PF}_6$  (Figure 1.6). Results have shown that the quenching mechanism, reductive or oxidative, of this reaction depends on the type of PS that is employed. When the reaction was carried out using the copper-based PS,  $[\text{Cu}(\text{dsbtmp})_2]\text{PF}_6$ , it followed the oxidative quenching pathway and the TON was a mere 35 ( $\text{H}_2/\text{Co}$ ) on average with a TOF of  $5 \text{ h}^{-1}$ . In contrast, with  $[\text{Ru}(\text{bpy})_3]_2\text{PF}_6$ , the reaction followed the more common reductive quenching process. Under these conditions the TON for this reaction dropped to 31  $\text{H}_2/\text{Co}$  with a TOF of  $17 \text{ h}^{-1}$ .<sup>25</sup>

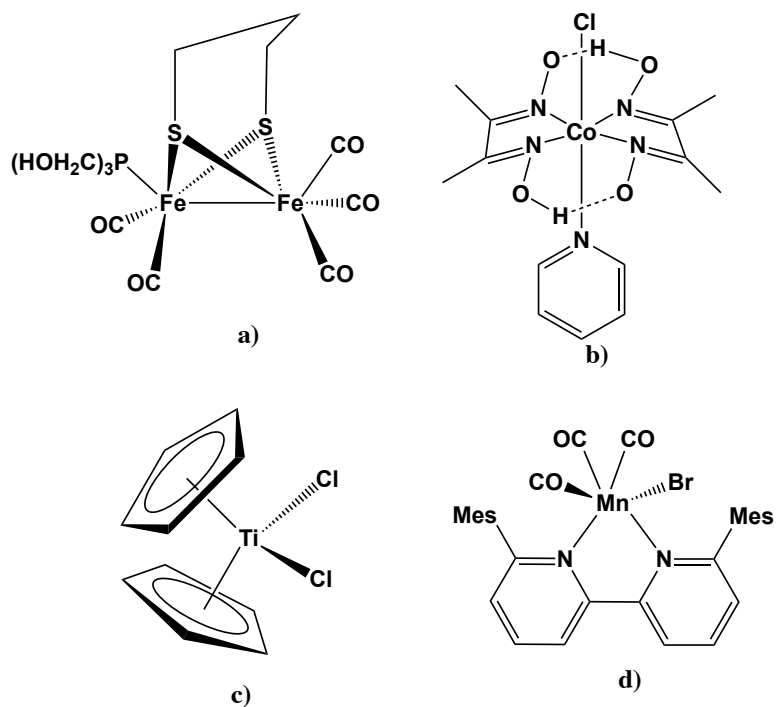


**Figure 1.5.** Some examples of active complexes for photocatalytic hydrogen production

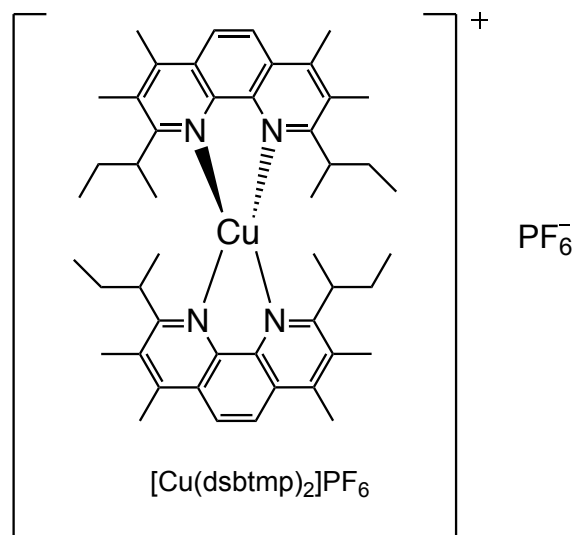


**Figure 1.6.**  $[Cu(dsbtmp)_2]PF_6$  Photosensitizer

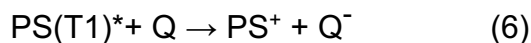
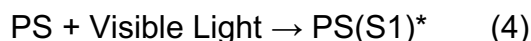
### Solvents (S)

Clearly, solvent will play a key role in a homogenous photocatalytic system. There are some organic solvents that are commonly used in most of the photocatalytic systems of

hydrogen production. These solvents include dimethylformamide (DMF), acetonitrile (ACN), dimethylacetamide (DMA), and methanol (MeOH).<sup>28</sup>

### Basic Mechanism of Photocatalytic Reactions

In general, the photocatalytic processes of many different reactions follow the same basic steps, which are now briefly outlined. The initial steps of the photocatalytic process can be expressed by the following equations.

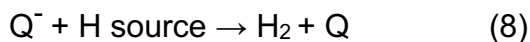


or

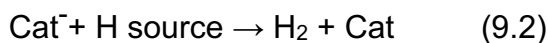


In these reactions PS is the photosensitizer, PS\* is the excited photosensitizer species, Q is the quenching molecule. Reaction 6 represents oxidative quenching and reaction 7 is for reductive quenching. The process begins when the photosensitizer, PS, absorbs a photon to be excited from the ground state (S0) to the first excited singlet state (S1). The singlet-excited state (S1) can then undergo intersystem crossing (ISC) to produce a longer-lived triplet-excited state (T1). Next, the energy will be transferred from the triplet state (T1) of the photosensitizer molecule to a quenching molecule (Q) and the photosensitizer will undergo electron energy transfer to end up as either the oxidized or reduced species with production of Q in the corresponding reduced or oxidized states and a chemical change will be resulted to the other molecule in the system. Q<sup>-</sup> in (6) is the catalyst which will react with the H source and will get oxidized (8). PS<sup>-</sup> in (7) will

transfer the electron to the catalyst (Cat in (9.1)) which then will be able to react with the hydrogen source (9.2).



or



### **Scope and Research Content of Thesis**

The previous material provides the general context and some literature background for the research carried out and described in this thesis. The results of this work are presented in the following two chapters which describe the original efforts in the exploration of two topics related to the chemistry of hydrogen, transfer hydrogenation and hydrogen production.

Chapter 2 began with the goal of discovering a new Fe-based catalyst for transfer hydrogenation of ketones. This project evolved to reveal that simple bases, namely commercial KO<sup>t</sup>Bu, is actually a very competent catalyst for these reactions.

A substantial change in topic is presented in Chapter 3 which describes efforts to discover a photocatalytic process for hydrogen production using a series of first row transition metals complexes with a well-known and easily prepared ligand, bis(methylthioether)pyridine. From these, the Fe complex was chosen to be the focus of this study as it showed a promising aptitude for photocatalytic hydrogen production from water.

## References

- 1 E. Knoevenagel and B. Bergdolt, *Chem. Berichte*, 1903, 2857–2860.
- 2 G. Brieger and T. J. Nestruck, *Chem. Rev.*, 1974, **74**, 567–580.
- 3 D. Wang and D. Astruc, *Chem. Rev.*, 2015, **115**, 6621.
- 4 T. R. B. Haddad, Y. M. Y.; Henbest, H. B.; Husbands, J.; Mitchell, *Proc. Chem. Soc.*, 1964, 361–365.
- 5 Y. Sasson and J. Blum, *Tetrahedron Lett.*, 1971, **24**, 2167–2170.
- 6 R. L. Chowdhury and J. E. Bäckvall, *J. Chem. Soc. Chem. Commun.*, 1991, **16**, 1063–1064.
- 7 F. Ok, M. Aydemir and F. Durap, *Appl. Organomet. Chem.*, 2014, **28**, 38–43.
- 8 R. Noyori, M. Yamakawa and S. Hashiguchi, *J. Org. Chem.*, 2001, **66**, 7931–7944.
- 9 E. J. Campbell, H. Zhou and S. B. T. Nguyen, *Org. Lett.*, 2001, **3**, 2391–2393.
- 10 A. Quintard and J. Rodriguez, *Angew. Chemie - Int. Ed.*, 2014, **53**, 4044–4055.
- 11 R. M. Bullock, *Science (80-. )*, 2013, **342**, 1054–1055.
- 12 D. Tavor, I. Gefen, C. Dlugy and A. Wolfson, *Synth. Commun.*, 2011, **41**, 3409–3416.
- 13 C. Sui-Seng, F. Freutel, A. J. Lough and R. H. Morris, *Angew. Chemie - Int. Ed.*, 2008, **47**, 950–943.
- 14 J.-X. Gao, T. Ikariya and R. Noyori, *Organometallics*, 2002, **15**, 1087–1089.
- 15 M. Perez, S. Elangovan, A. Spannenberg, K. Junge and M. Beller, *ChemSusChem*, 2017, **10**, 83–86.
- 16 A. M. Appel, J. E. Bercaw, A. B. Bocarsly, H. Dobbek, D. L. DuBois, M. Dupuis, J.

- G. Ferry, E. Fujita, R. Hille, P. J. A. Kenis, C. A. Kerfeld, R. H. Morris, C. H. F. Peden, A. R. Portis, S. W. Ragsdale, T. B. Rauchfuss, J. N. H. Reek, L. C. Seefeldt, R. K. Thauer and G. L. Waldrop, *Chem. Rev.*, 2013, **113**, 6621–6658.
- 17 British Petroleum, *Br. Pet.*, 2017, **66**, 1–49.
- 18 K. E. Dalle, J. Warnan, J. J. Leung, B. Reuillard, I. S. Karmel and E. Reisner, *Chem. Rev.*, 2019, **119**, 2752–2875.
- 19 P. D. Tran, L. H. Wong, J. Barber and J. S. C. Loo, *Energy Environ. Sci.*, 2012, **5**, 5902–5918.
- 20 N. S. Sickerman and Y. Hu, *Methods Mol. Biol.*, 2019, **1876**, 65–88.
- 21 G. Berggren, A. Adamska, C. Lambertz, T. R. Simmons, J. Esselborn, M. Atta, S. Gambarelli, J. M. Mouesca, E. Reijerse, W. Lubitz, T. Happe, V. Artero and M. Fontecave, *Nature*, 2013, **499**, 66–69.
- 22 F. Gärtner, B. Sundararaju, A. E. Surkus, A. Boddien, B. Loges, H. Junge, P. H. Dixneuf and M. Beller, *Angew. Chemie - Int. Ed.*, 2009, **48**, 9962–9965.
- 23 Z. Han, L. Shen, W. W. Brennessel, P. L. Holland and R. Eisenberg, *J. Am. Chem. Soc.*, 2013, **135**, 14659–13669.
- 24 R. S. Khnayzer, C. E. Mccusker, B. S. Olaiya and F. N. Castellano, *J. Am. Chem. Soc.*, 2013, **135**, 14068–14070.
- 25 Y. Yamazaki, H. Takeda and O. Ishitani, *Journal of Photochemistry and Photobiology C: Photochemistry Reviews*, 2015, **25**, 106–137.
- 26 S. P. Pitre, C. D. McTiernan, W. Vine, R. Dipucchio, M. Grenier and J. C. Scaiano, *Sci. Rep.*, 2015, **5**, 1–10.

27 S. Aoi, K. Mase, K. Ohkubo and S. Fukuzumi, *Catal. Sci. Technol.*, 2016, **6**, 4077–4080.

## Chapter 2

### Catalytic Transfer Hydrogenation in the Absence of a Transition Metal.

#### Potassium *tert*-Butoxide as a Simple and Effective MPV Catalyst for Ketone Hydrogenation.

##### Introduction

Hydrogenation of carbonyl compounds is one of the main reaction steps in pharmaceutical or food production industries. Transfer hydrogenation (TH) has been utilized for this transformation in large industrial scales.<sup>1</sup> One of the motivating factors for using TH methods is that they employ a simple to handle source for molecular hydrogen (e.g. 2-propanol or formic acid) rather than high pressures of flammable H<sub>2</sub> in the process. As described in Chapter 1, the last decades have focused on investigation and application of TH that has been dominated by Ru, Rh and Ir based complexes.<sup>2</sup> However, the cost and toxicity of these precious metals and their associated supporting ligands has become an increasing concern with regard to sustainability and environmental concerns.<sup>3</sup>

To address these issues, current research activities are increasingly focused on two approaches. The first avenue is the use of more earth-abundant first row transition metals such as Mn, Fe or Ni in place of the rare and potentially toxic heavier transition metals. For example, Fe is cheap and nontoxic, and complexes of Fe have been demonstrated to be active for TH reactions<sup>4</sup>. Importantly, successful catalytic complexes generally possess sophisticated supporting ligands that are required to achieve the desired activity. A second approach has been to explore the catalytic potential of the Meerwein, Ponndorf, and Verley (MPV) reaction using, for example, aluminum-based catalysts. The MPV method allows the hydrogen transfer to be carried out under mild temperature conditions.

However, the classical MPV conditions use aluminum alkoxide in stoichiometric or greater amounts.

The initial concept for the research in this chapter was to employ an Fe(II) pincer complex as a catalyst for the transfer hydrogenation of ketones. Initial results were quite promising but further investigations and use of control experiments revealed that the Fe complex was unnecessary and, to our surprise, that the bases used in the catalyst system were adequate for catalytic transformation. In this chapter we present a method allowing TH of aromatic and aliphatic ketones under mild conditions and in the presence of catalytic amounts of simple and economical alkali metal bases. Experiments that examined and established the best conditions for this reaction and an examination of the scope of this reaction using simple main group metal base species such as KO<sup>t</sup>Bu will be discussed.

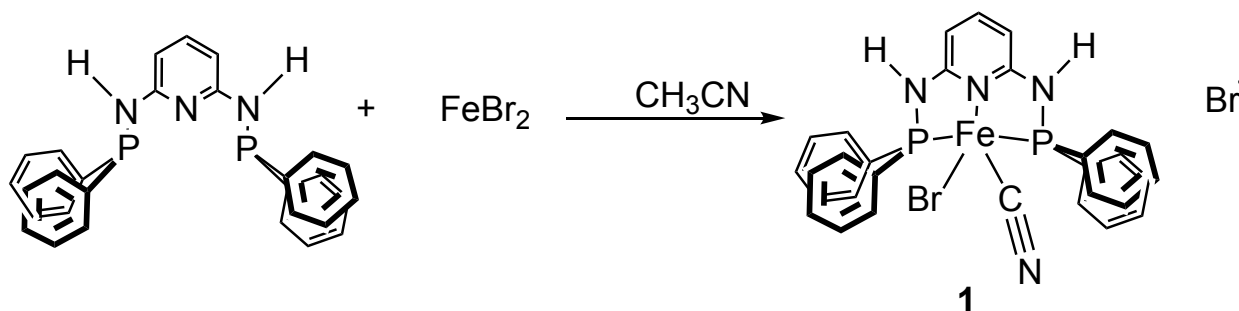
## **Results and Discussion:**

### **Investigation of the optimal reaction conditions for transfer hydrogenation of carbonyl compounds**

The reported success of Fe complexes for the TH process inspired the initiation of a project to explore the catalytic potential of Fe(II) complexes supported by a PNP pincer ligand. A pincer ligand is characterized by tridentate coordination that binds to metals in a planar, meridional mode. These ligands have been tailored to provide rigidity and stability in their metal complexes and can be rationally designed and constructed to organize the reaction pocket on a metal center thereby enabling enhanced control of the reaction pathways and products upon catalytic application.<sup>5</sup> The prototypical pincer ligand has an anionic central group (e.g. aryl ring), that is  $\sigma$ -bonded to the metal, with flanking neutral donors that link to the metal via chelate rings. The neutral ligand N,N'-

bis(diphenylphosphino)-2,6-diaminopyridine, 2,6-{Ph<sub>2</sub>PNR}<sub>2</sub>(NC<sub>5</sub>H<sub>3</sub>), has been employed in a number of transition metal complexes and the complex Fe{κ<sup>3</sup>-2,6-{Ph<sub>2</sub>PNH}<sub>2</sub>(NC<sub>5</sub>H<sub>3</sub>)}Br<sub>2</sub> (**1**) was targeted as a potential TH catalyst.

Our group had been exploring the use of these PNP pincers for a variety of redox reactions and this meant we had the ligand available for use in this project. In addition Kirchner et al<sup>4</sup> had reported preparation and characterization of related Fe(II) PNP pincer hydride complexes [Fe(2,6-{iPr<sub>2</sub>PNR}<sub>2</sub>(NC<sub>5</sub>H<sub>3</sub>))(H)(CO)(L)]<sup>n</sup> (R = H or Me) (L = Br<sup>-</sup>, CH<sub>3</sub>CN, pyridine, PMe<sub>3</sub>, SCN<sup>-</sup>, CO, or BH<sub>4</sub><sup>-</sup>; n = 0, +1). Some of these complexes were efficient catalysts for the hydrogenation of both ketones and aldehydes to alcohols under mild conditions, and for the complexes with the NMe spacers, they were chemoselective for hydrogenation of aldehydes. The mechanisms for these reactions were proposed to be an inner-sphere mechanism with insertion of the carbonyl group into a Fe-H bond. This reaction does not appear to proceed via a bifunctional mechanism.<sup>4</sup> We began by preparing the potential catalyst by the addition of 0.107 g of FeBr<sub>2</sub> which was dissolved in 5 ml CH<sub>3</sub>CN to 0.238 g of the 2,6-{Ph<sub>2</sub>PNH}<sub>2</sub>(NC<sub>5</sub>H<sub>3</sub>) ligand that was dissolved in 5ml DCM stirred for 18h at room T. Dark purple crystals when crystallized with EtOH/DEE at -30°C, allowed for a structural determination that definitively confirmed the formation of the complex shown in the Scheme 2.1.(Yield 0.295 g 85%)



**Scheme 2.1.** The divalent Fe complex with 2,6-{Ph<sub>2</sub>PNH}<sub>2</sub>(NC<sub>5</sub>H<sub>3</sub>) Br<sub>2</sub> Complex **1**

Complex **1** was fully characterized and single crystal X-ray analysis (Figure 2.1) confirmed the molecular structure shown in Scheme 2.1.

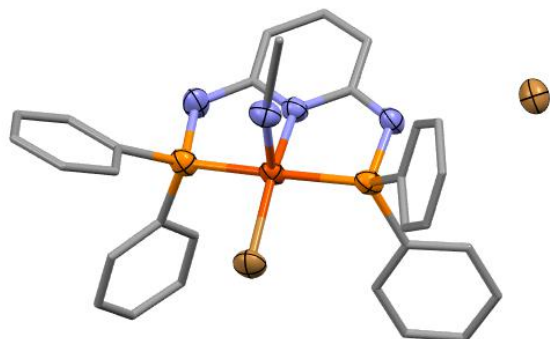
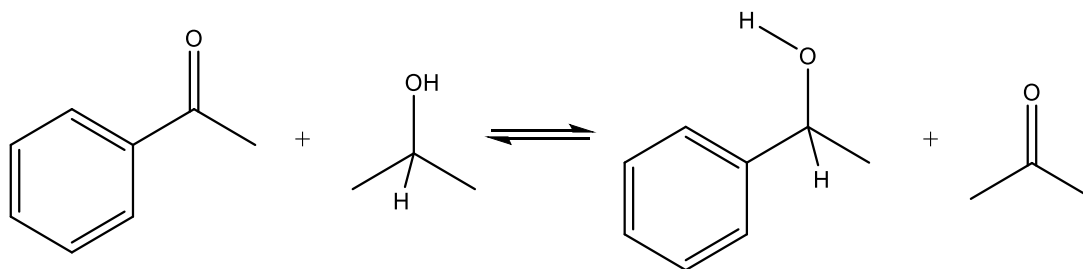


**Figure 2.1.** Crystal structure of Complex **1**

This species was then employed as a catalyst for the TH of acetophenone using 2-PrOH as the hydrogen source. The conditions used were 1 mM acetophenone, 1mol % of the complex **1**, 20mol% of the base KOtBu in 5ml of the 2-PrOH as both solvent and hydrogen source. As with most TH reactions, the addition of base is used to deprotonate the alcohol and form an MOR species. The presence of a  $\beta$ -hydrogen allows for an elimination reaction which can generate the MH intermediate state (Figure 1.3). Under these conditions we were pleased to observe a 99% conversion of acetophenone to the corresponding alcohol thus indicating an active TH catalyst system (Table 2.1).



**Scheme 2.2.** Benchmark reaction used in this chapter. Reagent: Acetophenone, Hydrogen donor/Solvent: 2-PrOH, Base: KOtBu, 24h, 80°C, Under N<sub>2</sub>

In order to more thoroughly examine the roles of catalyst and base, this same reaction was carried out with a variation of concentration of the Fe complex **1**. As can be seen in the Table 2.1, the first 3 entries show that the reaction showed excellent results as the concentration of **1** was reduced to lower concentrations. As a control experiment, we carried out the same reaction using simple FeBr<sub>2</sub> in place of complex **1**. The result of this experiment is shown as entry 4. To our surprise, the conversion for this reaction was as high as those using complex **1**. The first interpretation of this result was that there was no need for a ligand to support the Fe(II) center. As a control experiment, the same reaction was conducted only with 20 mol% of the KOtBu base. Surprisingly, this experiment yielded a 99% conversion in the absence of Fe. Although, alkali metal alkoxides have previously been used to mediate transfer hydrogenations, due to their low activity this reaction required a stoichiometric amount of base to accomplish product formation with a high conversion.<sup>6</sup> However, the interesting results presented above indicated that ketone reductions can be efficiently performed in the absence of other catalysts and with catalytic quantities of KOtBu. This is an important observation given that such strong bases are commonly added to transition metal catalyzed TH reactions throughout the literature.

**Table 2.1.** Experiments carried out to determine the activity of the iron complex **1** in the TH catalysis of acetophenone. All the reactions were performed under N<sub>2</sub> atmosphere in 5ml of refluxing 2-PrOH for 24h at 80°C.

Entry	Fe catalyst	Base	Results (Conversion%)
1	1mol% Complex <b>1</b>	20 mol%	99%
2	0.1mol% Complex <b>1</b>	20 mol%	99%
3	0.001mol% Complex <b>1</b>	20 mol%	99%
4	1mol% FeBr <sub>2</sub>	20 mol%	99%
5	-	20 mol%	99%

These results completely changed the focus of further TH investigations to elucidating the role of base in the TH reaction. To begin, the effectiveness of a range of different bases was examined by heating a 2-propanol solution of acetophenone in a sealed (under N<sub>2</sub> atmosphere) glass vial to 80°C for 24h. The results of these studies are given in Table 2.2.

As shown in Table 2.2, no TH reaction was observed in the presence of 20% K<sub>2</sub>CO<sub>3</sub> or Na<sub>2</sub>CO<sub>3</sub> at 80°C in 2-propanol (entries 1 and 2). K<sub>3</sub>PO<sub>4</sub> was able to promote the same reaction with 72% conversion within 24h. The transfer hydrogenation using 2-propanol also took place in the presence of other alkali hydroxides such as KOH and NaOH with a high conversion percentage as well as the organic base, Et<sub>3</sub>N. Results shown in Table 2.2, indicate that the order of reactivity was K<sub>3</sub>PO<sub>4</sub> < NEt<sub>3</sub> < NaOtBu = NaOH = KOH = KOtBu when 20mol% of the base was used.

This base catalyzed TH reaction would most likely follow the MPV mechanism. In fact, it is the basicity of the alkoxide anion in Al(OR)<sub>3</sub> catalysts that initiates the classical MPV reaction. It is also important to reiterate a key contrasting point of the classical MPV reaction and our observations shown in Table 2.2. Specifically, in general the MPV reaction proceeds in stoichiometric or greater than stoichiometric ratio of catalyst while the results reported here are at substoichiometric/catalytic ratios.

**Table 2.2.** Examining the effectiveness of different bases in a benchmark TH reaction shown in Scheme 2.2. Reactions were carried out for 24h at 80°C, in an N<sub>2</sub> atmosphere with 2.5ml 2-propanol.

Vial#	Base 20 mole %	Conversion %
1	K <sub>2</sub> CO <sub>3</sub>	No reaction
2	Na <sub>2</sub> CO <sub>3</sub>	No reaction
3	K <sub>3</sub> PO <sub>4</sub>	72
4	Triethylamine (NEt <sub>3</sub> )	84
5	NaOtBu	>99
6	NaOH	>99
7	KOH	>99

The results obtained with simple bases prompted a more detailed analysis of the literature in order to uncover studies for the role of base in TH reactions. Ouali et al have reported that NaOH and KOtBu are effective catalysts for similar reactions.<sup>7</sup> In that publication they also analyzed the bases used in the study for Table 2.2 The published results contrast with ours in that they indicated that NaOH and NaOtBu gave far superior reactivity compared to KOH and KOtBu. Polshettiwar and Varma reported that KOH at 25 mol% using 2-propanol was capable of catalyzing the MPV reaction at good (70% range) conversions.<sup>8</sup> In 2015, the NaOH catalyzed MPV hydrogenation of ketones was reinvestigated by Astruc and co-workers and some important contrasting results were obtained.<sup>9</sup> They determined that substoichiometric amounts of NaOH gave rather low conversions (e.g. 0.5 equiv of NaOH gave 23% conversion in 15 h) and that 2 equivalents of NaOH were required to get full conversion of ketone to alcohol. Given these conflicting results we chose to further investigate the capability of KOtBu in transfer hydrogenation.

The dependence of conversion on catalyst loading was also explored. Table 2.3 shows that in 24 hours, KO $t$ Bu loading from 5-20 mole % all gave complete conversion of acetophenone.

**Table 2.3.** The effect of different loadings of KO $t$ Bu on conversion for the reaction in Scheme 2.2. Reaction time was 24h at 80°C, under N<sub>2</sub>, with 2.5ml of 2-propanol.

Vial#	Base: KO $t$ Bu	Conversion%
1	5 mol%	99%
2	10 mol%	99%
3	20 mol%	99%

With these conditions defined, other reaction parameters were optimized. For this process the reaction shown in Scheme 2.2 was continued as a benchmark reaction. The model reaction was carried out in various alcoholic solvents (hydrogen sources), with KO $t$ Bu as catalyst at 80°C for 24 h. It was found that no reaction occurred in MeOH or EtOH. In addition, the use of another primary alcohol, n-BuOH, produced the desired product with the conversion of only 16%. On the contrary 2-PrOH proved to be the best choice for solvent and hydrogen source. It is well established that for this class of reactions, secondary alcohols are more effective than primary alcohols. It has been claimed that a suitable solvent for this reaction possess intermediate polarity and neither basic nor acidic properties. A comparison between aliphatic primary and secondary alcohols with the same carbon atom number should show that the secondary alcohol is a better hydrogen donor since aldehydes have lower reduction potentials than dialkyl ketones of the same carbon atom number. The best catalytic activity for acetophenone hydrogenation observed in 2-PrOH reflects essentially the ability of secondary alcohols for hydrogenating acetophenone via an additional reduction mechanism. The reactivity of different donors/acceptors is principally based on redox potential. This observation should

be true for both heterogeneous and homogeneous catalyst systems. Also, the hydrogen donor which is 2-PrOH is used as the solvent which according to the LeChatalier's principle, the equilibrium shifts to product.

Since the 24-hour reaction consistently gave a 99% conversion (Table 2.3), the effects of catalyst loading were not revealed. In order to examine catalyst loading it was necessary to reduce the reaction time to give only partial conversion. Thus, the transfer hydrogenation was analyzed after only 2 hours of reaction time using 2-PrOH (2.5 ml) as hydrogen source and solvent, in the presence of different concentrations of KO<sup>t</sup>Bu (5mol%- 70mol%) at 80°C. Results are shown in Table 2.4 and Figure 2.2. As expected, the conversion increased when higher amounts of base were loaded up to 30% providing 39% conversion. But surprisingly, with 50% and 70% for 2 hours the conversion decreased to 20% and 1% respectively. These results seem to indicate that the reaction actually slows down as the concentration of KO<sup>t</sup>Bu is increased. The current working hypothesis is that increasing concentration of KO<sup>t</sup>Bu may lead to clustering and bridging interactions around the K<sup>+</sup> cation centers which in turn interferes with the formation of the six-membered ring transition state for the MPV reaction.

**Table 2.4.** Conversion percent of 1-phenylethanol using different loading of KOtBu, condition: 1mmol Acetophenone, Time:2h, Temperature: 80°C, Under N<sub>2</sub>, Solvent: 2-propanol 2.5ml

Vial#	KOtBu (mol%)	Conversion%
1	5	0
2	10	7
3	20	26
4	30	39
5	50	20
6	70	1

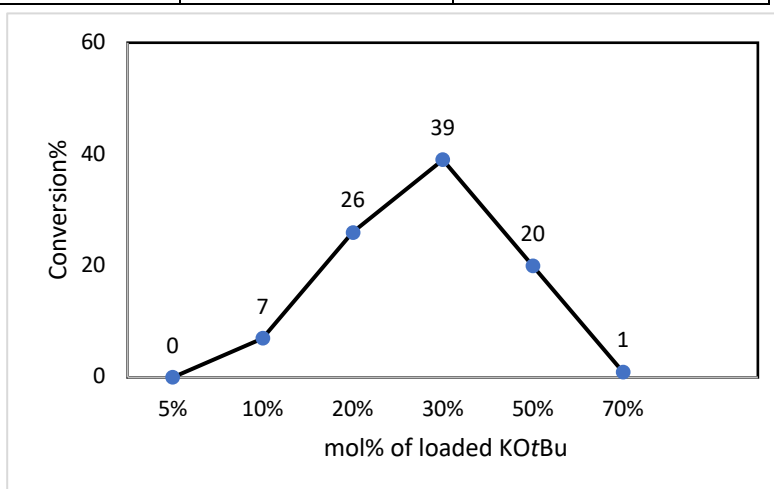


**Figure 2.2.** Graphical presentation of the results given in Table 2.3, showing the relation between the amount of catalyst in mol% and the conversion% for 2h.

The time profile of conversion of acetophenone with 10% catalyst loading is displayed in Figure 2.3. and Table 2.5. These reactions were carried out using 10 mol% of KOtBu as catalyst. Again, using the benchmark reaction of 1mmol of acetophenone in 2.5ml of 2-PrOH under a nitrogen atmosphere, these conditions showed a smooth conversion to 99% over a 24h time period.

**Table 2.5.** Conversion percent of 1-Phenylethanol for different reaction time using 1mmol acetophenone, 10 mol% KOtBu, in 2.5ml 2-PrOH for 24h, at 80°C, under N<sub>2</sub>.

Vial#	Time (h)	Conversion%
1	2	7
2	4	9
3	6	48
4	15	83
5	24	99

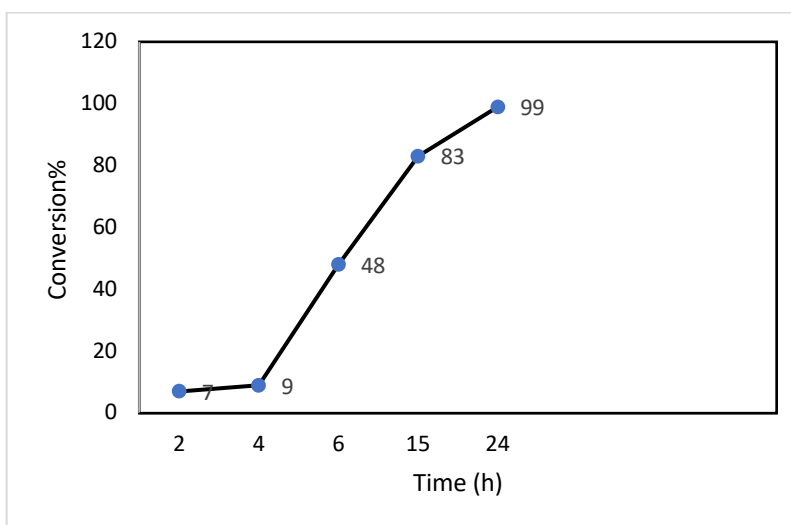


**Figure 2.3.** Graphical presentation of the results shown in Table 2.4, showing the relation between the reaction time and the conversion%.

The role of temperature on this reaction was also explored. The temperature was varied from 23°C to 80°C as shown in Table 2.6 with the data plotted in Figure 2.4. The secondary alcohol product (1-Phenylmethanol) was obtained with conversions of 0- 83% under these conditions when the reaction was conducted for 15h.

The induction period during the first 4h of reaction implies a transformation of the KOtBu into an active species. This may involve the transformation of the aggregation level of this salt and may also involve the conversion of KOtBu into KOiPr so that the catalytic cycle

can begin.

**Table 2.6.** The effect of temperature on the conversion percent of 1-Phenylethanol using 1mmol Acetophenone, 10mol% KOtBu, under N<sub>2</sub>, with 2.5ml 2-PrOH after 15h.

Vial#	Temperature (°C)	Conversion%
1	23	0
2	40	3
3	50	15
4	60	41
5	80	83

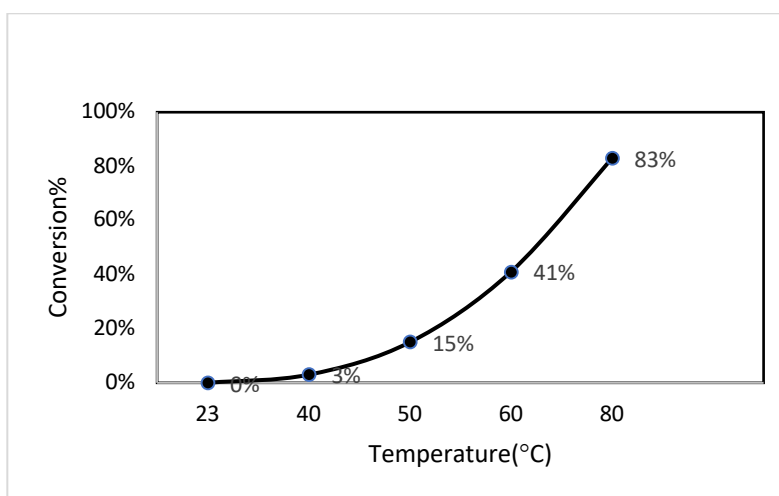


**Figure 2.4.** Graphical view of the data in Table 2.5, showing the relation between different temperatures and the conversion% for 15h.

In summary, the transfer hydrogenation was performed smoothly with 99% conversion under the optimal reaction conditions involving 2.5ml of 2-PrOH, 24h of reaction time, and 10 mol% of KOtBu, and 80°C. This result, associated with the mild reaction conditions is even competitive with transition metal-catalyzed transfer hydrogenation; most importantly, this catalytic system is superior regarding the economic and environmental issues. An increase in the temperature will increase the rate of the reaction.

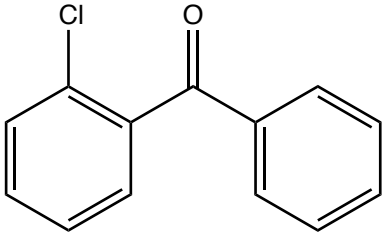
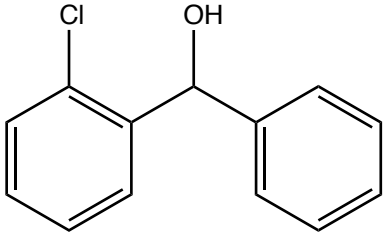
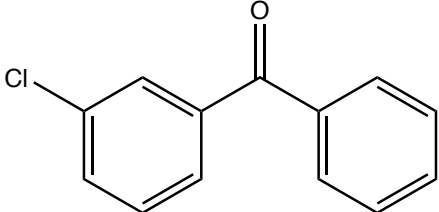
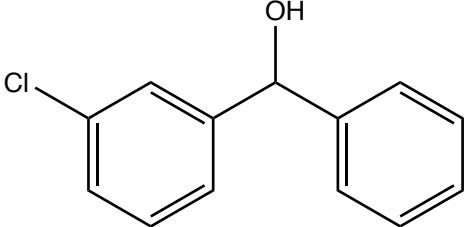
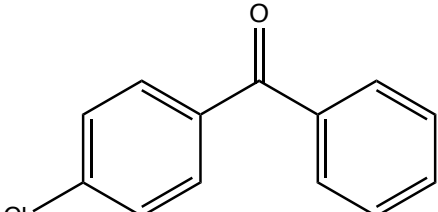
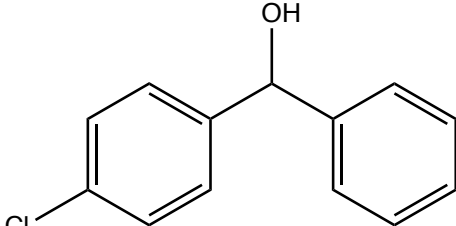
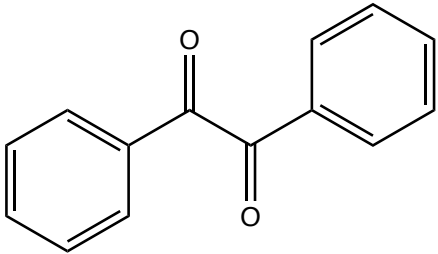
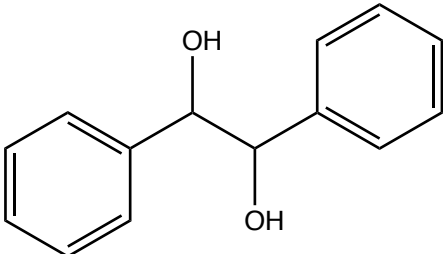
## Investigation of the substrate scope for transfer hydrogenation of carbonyl compounds using 2-PrOH as both solvent and hydrogen donor

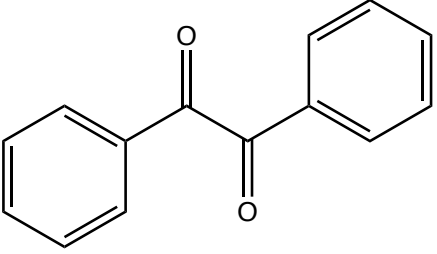
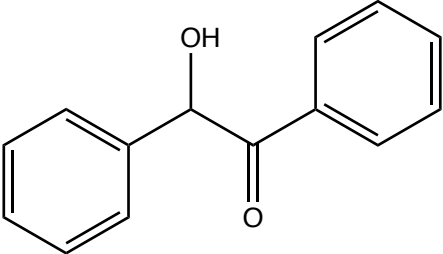
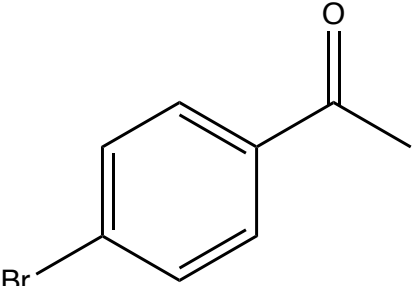
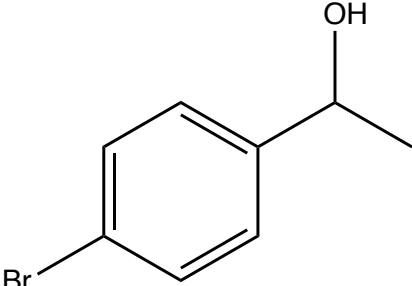
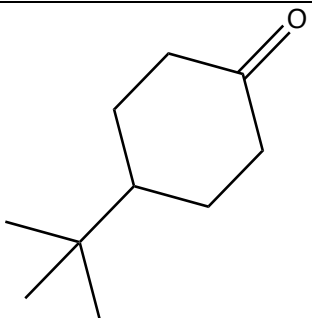
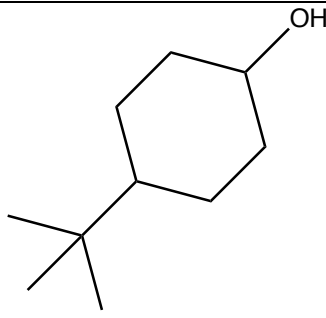
Encouraged by the efficiency of the reaction protocol described above, the scope of the transfer hydrogenation was examined with 10 mol% KO<sup>t</sup>Bu in 2-PrOH under a nitrogen atmosphere at 80°C for 24h, and the results are gathered in Table 2.7.

Results shown in the scope are consistent with the literature.<sup>7-9</sup> For example, when acetophenone bears electron-withdrawing substituents (e.g. Cl and Br) of the aromatic group in the para-position, the desired secondary alcohol was efficiently produced with 99% conversion (Table 2.7, entry 6 and 3). Moreover, ketones containing two aromatic substituents were also investigated; 4-Chlorobenzophenone was successfully hydrogenated by 2-PrOH with conversion of 98%. Electron withdrawing groups on ortho and meta positions of compound in entries 1 and 2 respectively caused a decrease in the conversion as electron withdrawing group (Cl) in *para* position of the same compound in entry 3 increased the conversion percent. This catalyst was also efficient for transfer hydrogenation of aliphatic ketones as can be seen in Table 2.7, entry 7 that 4-*tert*-butylcyclohexanone was converted to its corresponding alcohol by *cis/trans* (4-*tert*-butylcyclohexanone) 59/41%. The *trans* product is the thermodynamically more stable product due to the *tert*-butyl and alcohol OH groups both being in the equatorial positions. The equatorial position results in less steric crowding, and thus, it is favorable for larger substituents to occupy that position.<sup>10</sup> However, the *cis* product forms more rapidly due to the bulky *tert*-butyl group impeding the ability of the hydride ion to attack the top face of the molecule. But, a bulky group like KO<sup>t</sup>Bu is more probable to attack from bottom face of the 4-*tert*-butylcyclohexanone as the bulky *tert*-butyl group will hinder the hydride

attacking from the top face therefore in this method the *cis* product is more favorable than *trans* product.

**Table 2.7.** Substrate scope of carbonyl derivatives for KO<sup>t</sup>Bu-catalyzed transfer hydrogenation using 2-PrOH as hydrogen source and solvent

Entry	Ketone	Alcohol	Conversion%
1	 <p>2-Chlorobenzophenone</p>	 <p>2-Chlorobenzophenol</p>	23%
2	 <p>3-Chlorobenzophenone</p>	 <p>3-Chlorobenzophenol</p>	45%
3	 <p>4-Chlorobenzophenone</p>	 <p>4-Chlorobenzophenol</p>	98%
4	 <p>Benzil</p>	 <p>Hydrobenzoin</p>	41%

5	 <p>Benzil</p>	 <p>Benzoin</p>	14%
6	 <p>4'-Bromoacetophenone</p>	 <p>4'-Bromo-1-phenylethanol</p>	>99%
7	 <p>4-<i>tert</i>-Butylcyclohexanone</p>	 <p>4-<i>tert</i>-Butylcyclohexanol</p>	Cis/Trans: 59/41 %

## Experimental

### General Experimental Procedure:

1 mmol of the reagents and 20 mol% of KO<sup>t</sup>Bu were added to 2.5 ml of the solvent in a 15 ml glass vial which were sealed inside the glovebox. The vial was taken out of the glovebox and heated to the desired temperature with stirring and left for a specific amount of time. At the end of each reaction, after letting them cool down to the room temperature, the solvent was separated by vacuum techniques. NMR spectra of the products were

taken by dissolving the products in  $\text{CDCl}_3$ . The NMR spectra of all reagents and products are published and can be found in reliable databases.

### Calculation of the Conversion Percent

These conversion percent values are calculated using NMR data by comparing the ratio between specific peaks of reagent and the product.

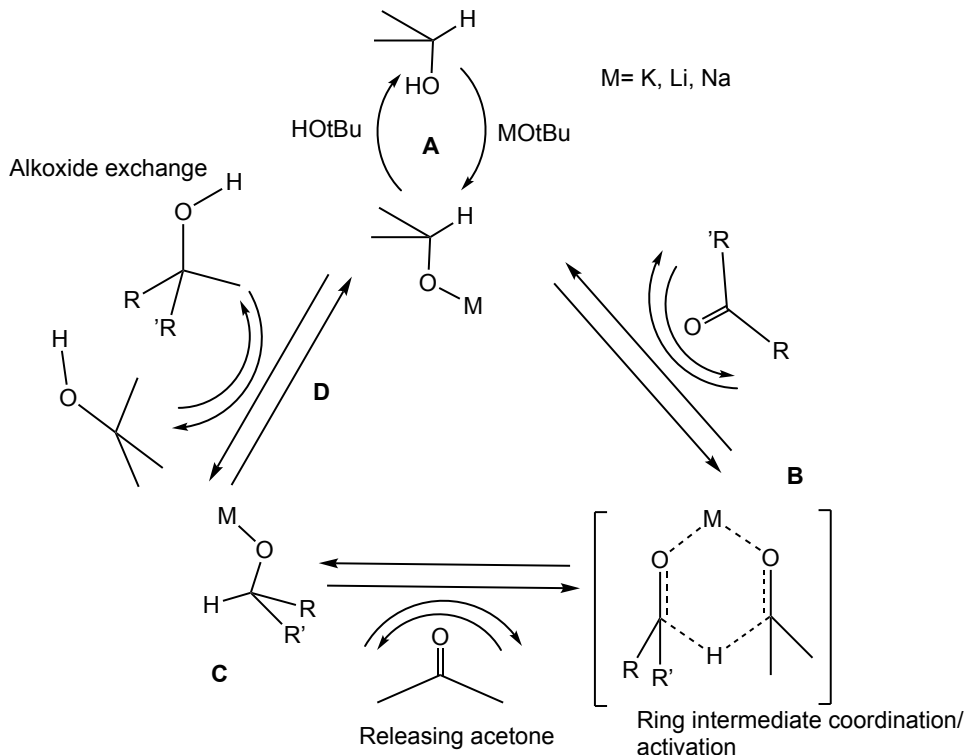
For example, for the benchmark reaction where acetophenone was converted to 1-phenyl ethanol, there is a singlet signal for the  $\text{CH}_3$  on acetophenone in the NMR which appears at 2.58 ppm and a doublet signal for the  $\text{CH}_3$  on 1-phenylethanol at 1.41 ppm. The ratio of the integral of these two signals ( $\text{Product}/\text{Reagent}$ ) into 100 will give us the conversion percent.

### Proposed Mechanism

To account for the base-catalyzed TH catalyzed hydrogenation of ketones, we propose a reversible catalytic cycle involving similar intermediates to those proposed for stoichiometric MPV reductions (Scheme 1.6). A first deprotonation of 2-propanol (**A**) would give the metal 2-propanoate species. Coordination of the ketone through the oxygen lone pair to the metal center can yield a cyclic intermediate (**B**). This six-membered species aligns the CH group of the alkoxide with the  $\delta^+$  C site of the coordinated ketone and provides a pathway for H transfer and release of acetone (**C**). The metal containing product is the resulting M-alkoxide which can react with 2-propanol (**D**; alkoxide exchange) to free the expected alcohol and regenerate the metal 2-propanoate. Steps b, c and d could be described as coordination/ activation and decoordination between the cation M (Lewis acid) and the ketone or alkoxide (Lewis base). In MPV reductions, strongly Lewis acidic Al(III) enables the formation of the Al

alkoxide (steps b and c), but the stability of the latter prevents the catalytic use of Al, and a hydrolysis is required in step d.

A key feature to consider for the metal is that the reaction rate is the combination of Lewis acidity of the metal ion and the exchange rate of the ligands. These two effects can be opposite each other. For example Al(III) will have a higher acidity but slower exchange rate. Metal ion ligand exchange rate may be a factor in catalytic activity. Al(III) is slower than Mg(II) and Ln(III) and it is very likely slower than for an alkali metal. However, the key reason for this is the rather low Lewis acidity of alkali metal cations. In fact, it was for these reasons that alkali metals with high exchange rate and low Lewis acidity were not perceived to be appropriate catalysts for the MPV reaction.



**Scheme 2.3.** Proposed mechanism for transfer hydrogenation of a ketone.

## **Future work**

These results demonstrated the ability of rather simple bases to act as excellent catalysts for transfer hydrogenation. In particular, success with KO $t$ Bu suggested that other commercial bases may function in an analogous catalytic manner. For example, we considered that Grignards, RMgX might be good sources for transition metal free catalysts. Examination of the catalytic ability of these species may reveal interesting effects of changing the main group metal identity from K<sup>+</sup> to Mg<sup>2+</sup>.

The initial experiments were performed with 20 mol% of MeMgBr<sub>2</sub> added to a mixture of 1mmol of acetophenone and 2.5ml of 2-PrOH under N<sub>2</sub> atmosphere heated for 24h up to 80°C, have shown promising results. 1-phenylethanol signal appeared in the NMR spectra with an approximate 87% conversion. More investigations can be followed in this area.

## **Conclusion**

In this chapter a simple method, using KO $t$ Bu as a catalyst for catalytic transfer hydrogenation was studied. The catalytic activity of this candidate was examined in different categories such as time, concentration, and temperature. The catalyst was successful in transfer hydrogenation of a variety of ketones into their corresponding alcohols. A key outcome from this work is that it highlights the active role of the base in TH reactions. Based on these results, care should be exercised in the analysis of transition metal/base catalyst systems.

## References

- 1 D. Wang and D. Astruc, *Chem. Rev.*, 2015, **115**, 6621.
- 2 N. Gorgas, B. Stöger, L. F. Veiros, E. Pittenauer, G. Allmaier and K. Kirchner, *Organometallics*, 2014, **33**, 6905–6914.
- 3 A. Ouali, J. P. Majoral, A. M. Caminade and M. Taillefer, *ChemCatChem*, 2009, **1**, 504–509.
- 4 N. Gorgas, B. Stöger, L. F. Veiros and K. Kirchner, *ACS Catal.*, 2016, **6**, 2664–2672.
- 5 H. Valdés, M. A. García-Eleno, D. Canseco-Gonzalez and D. Morales-Morales, *ChemCatChem*, 2018, **10**, 3136–3172.
- 6 M. D. Le Page and B. R. James, *Chem. Commun.*, 2000, 1647–1648.
- 7 J. Ballester, A. M. Caminade, J. P. Majoral, M. Taillefer and A. Ouali, *Catal. Commun.*, 2014, **47**, 58–62.
- 8 V. Polshettiwar and R. S. Varma, *Green Chem.*, 2009, **11**, 1313–1316.
- 9 D. Wang, C. Deraedt, J. Ruiz and D. Astruc, *J. Mol. Catal. A Chem.*, 2015, **400**, 14–21.
- 10 and P. D. Michael Novak\*, Benjamin W. Gung, James W. Hershberger, Richard T. Taylor, Bright Emenike, Mrinal Chakraborty, Ashley N. Scioneaux, Amanda E. Ponsot, *Chem. Educ.*, 2009, **14**, 232–235.

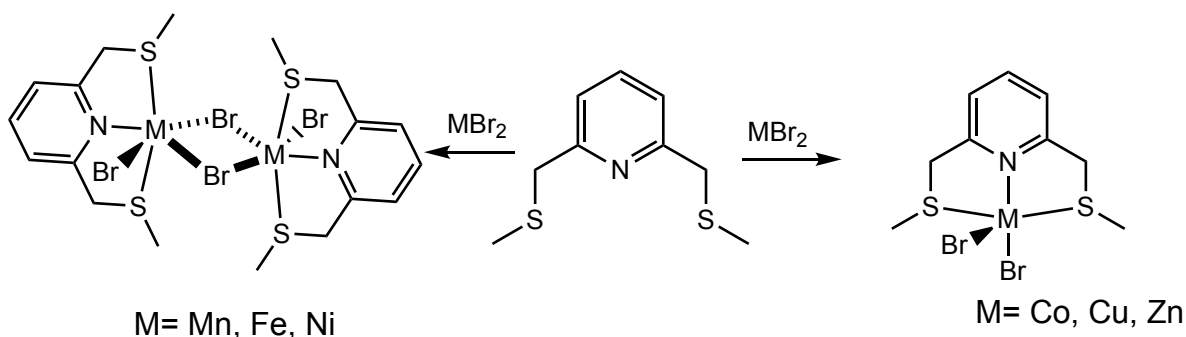
## Chapter 3

### Photocatalytic Hydrogen Production using Earth-Abundant Metal Catalysts with Unprecedented Coordination Environments

#### Introduction

The advancement of inorganic and organometallic chemistry has been closely linked with the constant development of supporting ligand environments. Among the sizable classes of ligands employed in support of transition metals, pincer-type architectures represent a large category with well-established importance.<sup>1</sup> Pincer-type architectures, as introduced in Chapter 2, represent an important class of ligand frameworks for the design and synthesis of transition metal coordination complexes and catalysts. In particular, we were interested in bis(thioether) ligands displaying an “SNS” coordination array. While the first complexes with these ligands were reported for Cu(II) in 1976<sup>2</sup>, this framework, particularly for earth-abundant metals, has received less and more infrequent attention compared to similar pincer donor arrays. To date, pyridyl-centered, bis(thioether) SNS complexes have been reported for the first-row metals from Fe to Zn and for some of the heavier congeners of these metals. New interest in ligands with thioether centers has been stimulated by a report that related thioether ligands form well-defined ethylene trimerization catalysts with Cr(III) as well as the potential for hemilabile bonding,<sup>3</sup> between the coordinated metal center and the hard nitrogen donor and soft sulfur donor atoms. The application of bis(thioether)pyridine SNS ligands in molecular transformations and catalysis is beginning to be revealed. In addition to stoichiometric reactions,<sup>4</sup> there have been investigations of catalytic transformations that have included oxidation reactions,<sup>5</sup> C-S coupling reactions,<sup>6</sup> and catalyzed formation of cyclic carbonates from CO<sub>2</sub> and

epoxides.<sup>7</sup> In an effort to explore more systematically the catalytic potential of this ligand scaffold, a series of divalent first row transition metal complexes of the simple archetypal neutral SNS pincer, 2,6- (CH<sub>3</sub>SCH<sub>2</sub>)<sub>2</sub>C<sub>5</sub>H<sub>3</sub>N were prepared. This series of earth-abundant metals yielded new complexes with the empirical formulae M( $\kappa^3$ -2,6- (CH<sub>3</sub>SCH<sub>2</sub>)<sub>2</sub>C<sub>5</sub>H<sub>3</sub>N)Br<sub>2</sub> (M = Mn, Fe, Co, Ni, Cu, Zn) displaying tridentate ligand coordination and a range of five- and six-coordinate species (Scheme 3.1). Analysis of the resulting complexes reveals a set of monomeric and dinuclear species, whose coordination mode is associated with a delicate balance of structural features arising from the metal's d orbital occupancy and the steric load of the ligand. Dimerization of the solid-state structure appears to be primarily favored through lower steric load from the ligand and lower metal d-electron count.<sup>8</sup> This series provided a platform to explore a range of catalytic potential and in this chapter, an attempt to study the photocatalytic ability of these complexes for H<sub>2</sub> production using photochemical reactions was studied.



**Scheme 3.1.** Summary of metal bis(thioether) pyridyl complexes used in this study.

Chapter 1 gave a general description of the important components and parameters that require attention and consideration in order to study the photocatalytic ability of this set of first row metal complexes for hydrogen generation. For example, two main components for a photocatalytic system are the photosensitizer and the catalyst. The photosensitizer

is responsible for the light absorption to generate an excited state photosensitizer that can use the absorbed energy for the reaction. Perhaps the most well-known and common species that has been used in this regard is the Ru(II) complex,  $[\text{Ru}(\text{bpy})_3]^{2+}$ . The success of this photosensitizer is due to its unique combination of chemical stability, redox properties, and long lifetime of the excited state. The catalyst component is the central exploration and discovery target in this thesis. The next most obvious components that need consideration are the electron donor and the reaction solvent. Recall that an electron donor is required to provide the electrons needed in the reduction reaction and this species most commonly interacts with the excited state photosensitizer to undergo an electron transfer quenching of this species. There are a variety of different quenchers that have been used as the electron donor in hydrogen photoreduction systems. Examples include triethanolamine (TEOA), triethylamine (TEA), 1-benzyl-1,4-dihydronicotinamide (BNAH), and sodium ascorbate (NaA). In terms of solvent, once again a variety have been employed in successful photoreactions. These include, dimethylformamide (DMF), acetonitrile (ACN), dimethylacetamide (DMA), and methanol (MeOH).<sup>9</sup>

In summary, the photocatalytic hydrogen reduction system will generally consist of a catalyst, photosensitizer, sacrificial electron donor, and solvent. This reaction mixture will then be subject to irradiation from a light source which can be characterized by emission wavelength and photon flux/intensity.

## Results and Discussion

With the series of compounds shown in Scheme 3.1 in our hands, their potential for catalytic hydrogen generation, using water as the hydrogen source, was investigated. A set of initial experiments was done while a mixture of 1mmol of complex and photosensitizer,  $[\text{Ru}(\text{bpy})_3](\text{PF}_6)_2$ , in 4ml of reaction solvent (DMF), 0.2ml water, and 1ml TEOA was stirred under the irradiation of LED light (405nm) under  $\text{N}_2$  atmosphere for 24h. These were selected to allow some analysis of the scope and employed a common set of conditions based on the literature. The initial results of this exploration are presented in Table 3.1, showing that the catalyst was able to produce hydrogen from water.<sup>10</sup>

**Table 3.1.** Photochemical  $\text{H}_2$  generation from water for the series  $\text{M}(\kappa^3\text{-}2,6\text{-}(\text{CH}_3\text{SCH}_2)_2\text{C}_5\text{H}_3\text{N})\text{Br}_2$  ( $\text{M} = \text{Mn, Fe, Co, Ni, Cu, Zn}$ ). All reactions employed 1mmol of complex and photosensitizer,  $[\text{Ru}(\text{bpy})_3](\text{PF}_6)_2$  in 4ml of reaction solvent (DMF) with 0.2ml of added water. The electron donors, triethanolamine (TEOA), triethylamine (TEA) and 1-Benzyl-1,4-dihydronicotinamide (BNAH) were employed. Irradiation with 405 nm LED light conducted under an  $\text{N}_2$  atmosphere for 24 h.

Complex	ED	$\text{H}_2$ $\mu\text{mol}$
$[\text{Mn}\{\kappa^3\text{-}2,6\text{-}(\text{MeSCH}_2)_2\text{NC}_5\text{H}_5\}\text{Br}_2]_2$	TEOA	88
	TEA	4
	BNAH	5
$[\text{Fe}\{\kappa^3\text{-}2,6\text{-}(\text{MeSCH}_2)_2\text{NC}_5\text{H}_5\}\text{Br}_2]_2$	TEOA	133
	TEA	15
	BNAH	28
$\text{Co}\{\kappa^3\text{-}2,6\text{-}(\text{MeSCH}_2)_2\text{NC}_5\text{H}_5\}\text{Br}_2$	TEOA	58
	TEA	31
	BNAH	16
$\text{Ni}\{\kappa^3\text{-}2,6\text{-}(\text{MeSCH}_2)_2\text{NC}_5\text{H}_5\}\text{Br}_2$	TEOA	194
	TEA	36
	BNAH	51
$\text{Cu}\{\kappa^3\text{-}2,6\text{-}$	TEOA	84
	TEA	6

$(\text{MeSCH}_2)_2\text{NC}_5\text{H}_5\text{Br}_2$	BNAH	12
$\text{Zn}\{\kappa^3\text{-2,6-}(\text{MeSCH}_2)_2\text{NC}_5\text{H}_5\text{Br}_2$	TEOA	4
	TEA	3
	BNAH	4
No Catalyst	TEOA	-

The best results for the  $\text{H}_2$  production were with  $[\text{Fe}\{\kappa^3\text{-2,6-}(\text{MeSCH}_2)_2\text{NC}_5\text{H}_5\text{Br}_2\}_2$  and  $[\text{Ni}\{\kappa^3\text{-2,6-}(\text{MeSCH}_2)_2\text{NC}_5\text{H}_5\text{Br}_2\}_2$ . The iron complex was particularly interesting due to the fact that Fe is the most abundant metal in earth's crust, it is cheap, and non-toxic.

As mentioned in Chapter 1, a photochemical reaction contains several integrated components that consist of a catalyst, photosensitizer, electron donor, substrate and the solvent. In order to optimize for the photocatalytic  $\text{H}_2$  generation each component was varied. All of the reactions used a photosensitizer and were done under  $\text{N}_2$  for 24h while an LED light with 405 nm of wavelength was conducted on them. The formation of  $\text{H}_2$  was analyzed using GC-mass spectrometry.

### Variation of Electron Donors

An electron donor is required for this photoreduction and several different donors were explored under standard condition. The first three donors are amines with known activity in photocatalytic reduction reactions. TEOA is perhaps the most commonly used ED. For this analysis,  $\text{Ru}(\text{bpy})_3^{2+}$  and DMF were used as photosensitizer and solvent, respectively. The results from the different electron donors are summarized in Table 3.2. Of the four electron donors employed in this study, TEOA was superior and chosen for further optimization.

**Table 3.2.** Photochemical H<sub>2</sub> generation using [Fe{κ<sup>3</sup>-2,6-(MeSCH<sub>2</sub>)<sub>2</sub>NC<sub>5</sub>H<sub>5</sub>}Br<sub>2</sub>]<sub>2</sub> as catalyst. All reactions were carried out with 1mmol of complex and photosensitizer, [Ru(bpy)<sub>3</sub>](PF<sub>6</sub>)<sub>2</sub> in 4ml of DMF with 0.2ml of added water and conducted under an N<sub>2</sub> atmosphere for 24 h. Irradiation wavelength was 405 nm. a) 1ml, b) 0.2 mg 1-Benzyl-1,4-dihydronicotinamide (BNAH)

Electron donor	H <sub>2</sub> (μmol)	TON
TEOA (N(CH <sub>2</sub> CH <sub>2</sub> OH) <sub>3</sub> ) <sup>a</sup>	73	18.25
NEt <sub>3</sub> <sup>a</sup>	14	3.5
DMT <sup>a</sup>	0	0
BNAH <sup>b</sup>	0	0

### Variation of Solvent

Once TEOA was selected as the preferred ED, the effect of solvent was explored. Four different solvents were selected with the choice based on the fact that these solvents are common in photocatalytic reactions such as CO<sub>2</sub> reduction or hydrogen production.<sup>11</sup>

Results from the impact of different solvents are presented in Table 3.3.

All four solvents selected for this investigation proved to be effective with DMF showing superior performance. The polarity of DMF is 6.4 which is higher than THF (4.0) and CH<sub>3</sub>CN (5.8) and a little lower than DMA (6.5) which suggests that polarity may play an important role in this reaction.

**Table 3.3.** Photochemical H<sub>2</sub> generation from water using [Fe{κ<sup>3</sup>-2,6-(MeSCH<sub>2</sub>)<sub>2</sub>NC<sub>5</sub>H<sub>5</sub>}Br<sub>2</sub>]<sub>2</sub>. All reactions were carried out with 1mmol of complex and photosensitizer, [Ru(bpy)<sub>3</sub>](PF<sub>6</sub>)<sub>2</sub> in 4ml of reaction solvent and 1ml TEOA with 0.2ml of added water conducted under an N<sub>2</sub> atmosphere for 24 h. Irradiation wavelength was 405nm.

Solvent	H <sub>2</sub> (μmol)	TON
DMF	73	18.3
DMA	45.2	11.3
THF	43.7	10.9
Acetonitrile	35	8.8

## Variation of Photosensitizers

The photosensitizer is a key component and  $\text{Ru}(\text{bpy})_3^{2+}$  is the most commonly employed in the literature due to its unique combination of chemical stability, redox properties, and long lifetime of the excited state. It is an orange compound that can absorb light better than a white or very slightly colored compounds, and its excited state life time is 1100 ns.<sup>12</sup> As seen in Table 3.4, the  $\text{Ru}(\text{bpy})_3^{2+}$  was quite effective in this reaction. In order to explore the possibility of removing Ru, two organic dyes that have been established to function as sensitizers in photocatalytic reduction were also explored. Table 3.4 presents a summary of the results for different photosensitizers.

**Table 3.4.** Photochemical  $\text{H}_2$  generation from water using  $[\text{Fe}\{\kappa^3\text{-2,6-(MeSCH}_2)_2\text{NC}_5\text{H}_5\}\text{Br}_2\}_2$ . All reactions were carried out with 1mmol of complex and photosensitizer, in 4mL of DMF and 1ml TEOA as the ED with 0.2ml of added water conducted under a  $\text{N}_2$  atmosphere for 24 h. Irradiation wavelength was 405nm.

Photosensitizer	$\text{H}_2$ ( $\mu\text{mol}$ )
$[\text{Ru}(\text{bpy})_3](\text{PF}_6)_2$	73
Eyosin-Y	0
Purpurin	0

As can be seen in Table 3.4.,  $[\text{Ru}(\text{bpy})_3](\text{PF}_6)_2$  was the active photosensitizer which can be because it can absorb the irradiated wavelength which was 405nm whereas Purpurin absorption peak is around 695 nm and Eyosin-Y is around 526 nm<sup>13</sup>.

## Emission-Quenching Experiments

Since the photochemical process involves the transfer of energy from the excited state photosensitizer ( $\text{PS}^*$ ) to another agent, commonly the electron donor, emission quenching experiments using the electron donor (Figure 3.1) and catalyst (Figure 3.2) molecules were carried out according to a similar procedure in the literature.<sup>14</sup> A solution

of the photosensitizer  $\text{Ru}(\text{bpy})_3(\text{PF}_6)_2$  (0.1 mM) in anhydrous acetonitrile was prepared and mixed with different concentrations of the quencher. For example, using the electron donors, TEOA, the concentration was varied from 0 mM to 3.75 mM as shown in Figure 3.1. The steady-state emission spectrum (excitation wavelength 450 nm) of each solution was recorded, and the intensity of the luminescence for the  $^3\text{MLCT}$  excited state of the photosensitizer (452 nm) was recorded.

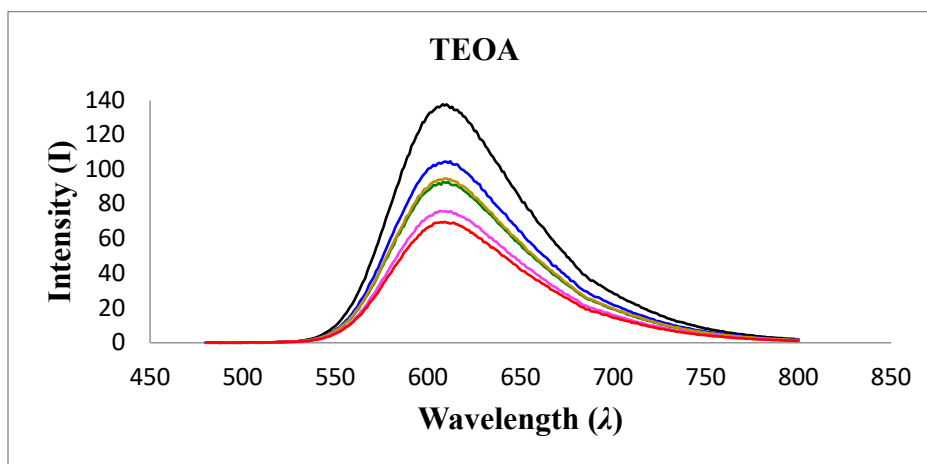


**Figure 3.1.** Spectra demonstrating the quenching of the emission from the photosensitizer  $\text{Ru}(\text{bpy})_3(\text{PF}_6)_2$  with various concentrations (0-3.75 mM) TEOA.

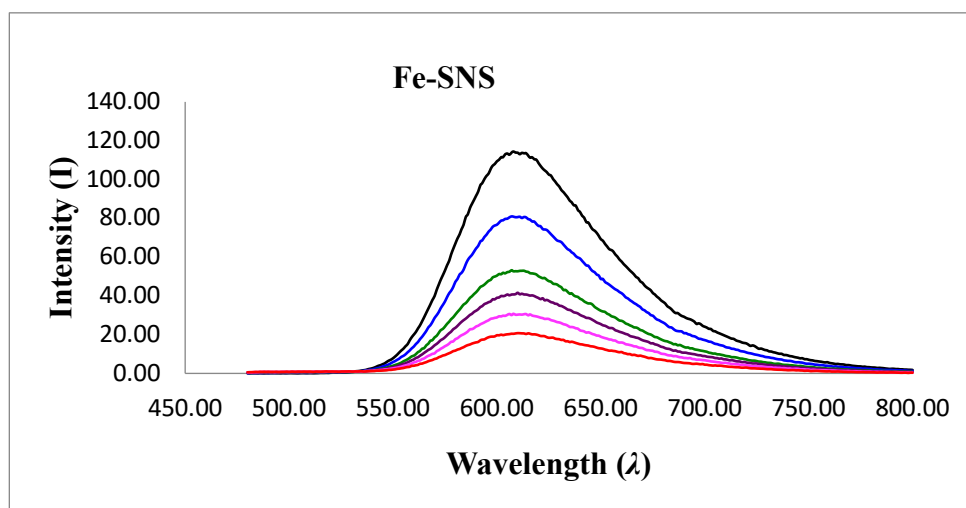


**Figure 3.2.** Spectra demonstrating the quenching of the emission from the photosensitizer  $\text{Ru}(\text{bpy})_3(\text{PF}_6)_2$  with various concentrations (0-0.6mM) Fe-SNS complex.

As expected, the quenching experiment results support the fact that TEOA does quench the photosensitizer as was mentioned in the literature.<sup>14</sup> More surprisingly, these experiments also document that the catalyst also quenches the photosensitizer although it was weaker than TEOA. All this can help us to better understand if the electron transfer follows a reductive or oxidative quenching mechanism.

### Study of the effect of the amount of catalyst and photosensitizer

A study on the effect of the Cat:PS was done in order to better understand how the productivity of the system depends on the amount of catalyst and photosensitizer and also to see which one is the limiting species. The results are given in Table 3.5.

**Table 3.5.** Photochemical H<sub>2</sub> generation from water using [Fe{κ<sup>3</sup>-2,6-(MeSCH<sub>2</sub>)<sub>2</sub>NC<sub>5</sub>H<sub>5</sub>}Br<sub>2</sub>]<sub>2</sub>. All reactions were carried with complex and photosensitizer, in 4ml of DMF and 1ml TEOA with 0.2ml of added water conducted under an N<sub>2</sub> atmosphere for 24 h. Irradiation wavelength was 405nm.

Catalyst (mmol)	Photosensitizer (mmol)	H <sub>2</sub> (μmol)
1	1	73
0.5	1	39
0.5	0.5	27

According to the results given in the Table 3.5, the outcome of the reaction is more influenced by the amount of catalyst than by the amount of photosensitizer. This suggests that the reaction mechanism depends on a reductive quenching process, because, the amount of TEOA is very high (1ml) and higher amounts of PS will result in great amounts of reduced PS which will be delivered to the catalyst. But when we change the amount of the catalyst concentration, there is no change in the amount of produced hydrogen, because no matter how much we increase the amount of PS the catalyst still accepts a limited number of electrons. For example, when Cat:PS was 0.5:1 the yield dropped by

almost half and the decrease in the amount of PS did not change the outcome significantly in the case of 0.5:1. To better prove this idea a reaction with 0.5:2 must be done.

### Time profile of the catalytic reaction

Catalyst productivity over time was measured for 72 h. Results are given in Table 3.6.

**Table 3.6.** Results from different time of irradiation of LED light.

Time (h)	H <sub>2</sub> (μmol)
0	0
24	73
48	104
72	118

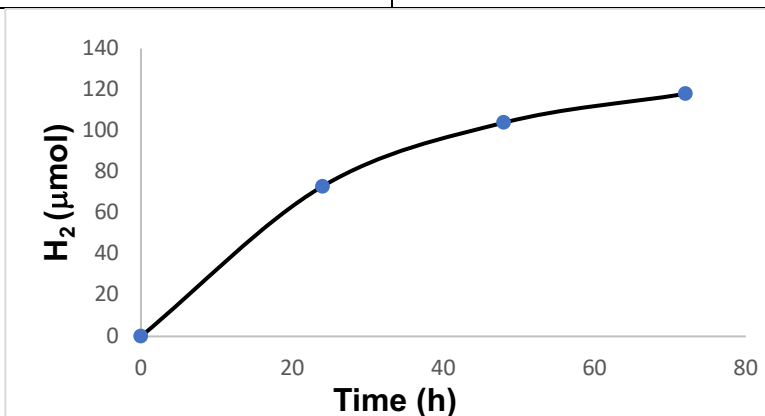


**Figure 3.3.** Graphical presentation of the results shown in Table 3.6, showing the relation between the productivity of the catalyst and Time.

In Figure 3.3, a smooth curve can be seen which means the catalyst was still productive and stable with some limit to the production after 72h. A change in the color of the solution from transparent orange to dark brown can possibly be a result of decomposition of the catalyst or the photosensitizer which can in turn lead to decreased productivity of the system.

## Blank reactions

With an optimized set of experimental parameters, a set of blank experiments were carried out in order to ensure the necessity of each component for this system. Essentially, each component of the reaction system was removed and the amount of generated H<sub>2</sub> was determined. The results are shown in Table 3.7.

**Table 3.7.** Blank reactions. Each reaction was done under N<sub>2</sub> atmosphere for 24h with irradiation wavelength of 405nm.

Component	H <sub>2</sub> (μmol)
No Catalyst	0
No Photosensitizer	0
No ED	0
No Water	138

As expected, each of the components was necessary for effective catalysis. However, the final entry in this table (138 is the average of 142.7, 139.8, 133.4. these experiments were done in the same condition to decrease the errors and test the reproducibility) was not what was expected. This indicated that the system was actually more productive in the absence of water. This was surprising since the initial and the optimization experiments were based on the assumption that the protons that were reduced to make the observed H<sub>2</sub> were derived from water. In fact, it would appear that water actually had a detrimental effect on H<sub>2</sub> production with TEOA as the electron donor. To make clearly examine this situation, a set of standard reactions with different amounts of water were carried out with the results presented in Table 3.8.

**Table 3.8.** Results from addition of different amounts of water on the photochemical H<sub>2</sub> production.

Water (ml)	H <sub>2</sub> (μmol)
0.1	63
0.2	73
0.5	53
1	52

As can be seen in Table 3.8. Increasing the amount of water resulted in decreased hydrogen production. Furthermore, a reaction was carried out with added D<sub>2</sub>O and the results from mass spectrometry showed only H<sub>2</sub> with no evidence of DH or D<sub>2</sub>. These results also point to the fact that water is not the source of H<sub>2</sub>.

#### **Calculation of the Standard deviation:**

Based on the reactions done without water in the system for 3 times, the standard deviation is calculated as 4.5 using the equation (1) below. Within the standard deviation, numbers in the Table 3.8 are the same.

$$s = \sqrt{\frac{1}{N-1} \sum_{i=1}^N (x_i - \bar{x})^2} \quad x = \{142.7, 139.8, 133.4\} \quad (1)$$

This can be as a result of an acid base reaction between water and the electron donor so then the water will not participate in the main reaction also it will reduce the amount of involved ED in the main hydrogen production system.

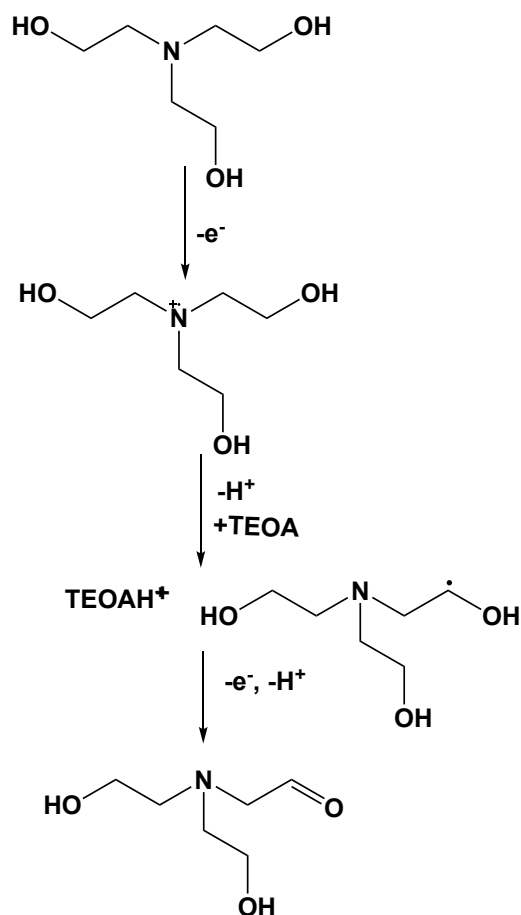
We thought that the only component that can be the hydrogen source in these series of reactions is the ED. To explore this idea, reactions with TEOA and NEt<sub>3</sub> were repeated without any added water and the results shown in Table 3.9. These data support the idea

that the hydrogen source was the ED. Although that there is not a noticeable difference for  $\text{NEt}_3$ . TEOA proved to be the best choice as maybe its OH groups can be good source of hydrogen.

**Table 3.9.** Results of the photochemical reaction with no water in the presence of the reactive ED.

Electron donor	$\text{H}_2$ ( $\mu\text{mol}$ )
TEOA ( $\text{N}(\text{CH}_2\text{CH}_2\text{OH})_3$ )	138
$\text{NEt}_3$	15

As there is no water in the system, the degradation of TEOA can happen as shown below (Scheme 3.2) which will release 2 electrons and 2  $\text{H}^+$ .



**Scheme 3.2.** Degradation of TEOA

### Varying the amount of added TEOA

We studied the effect of changing the concentration of TEOA on the amount of produced hydrogen as well, and the results are given in Table 3.10. The amount of generated H<sub>2</sub> increased with increasing the amount of TEOA.

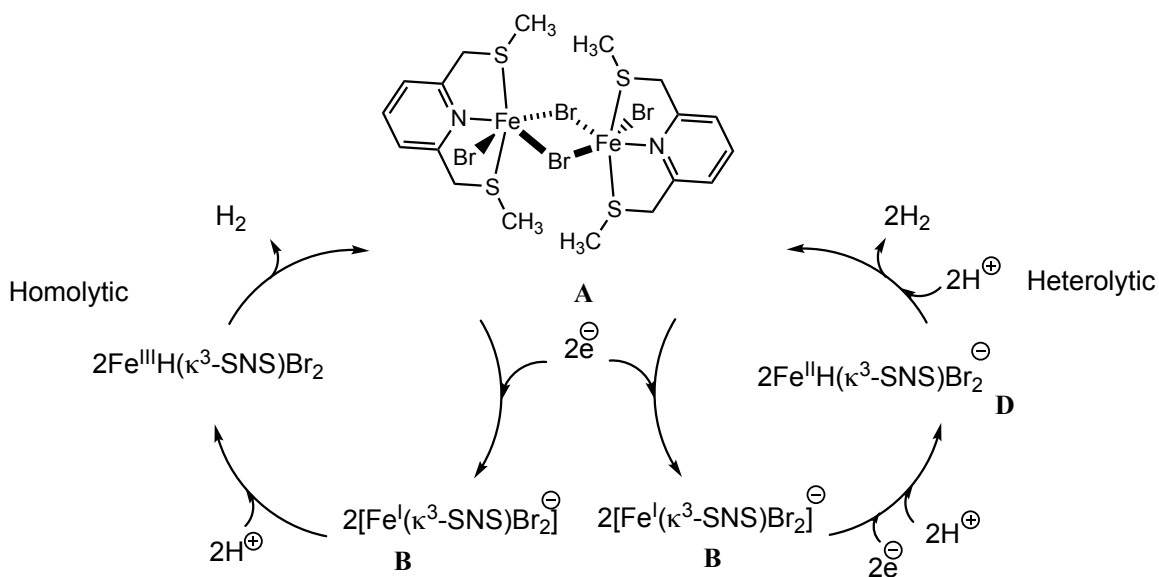
**Table 3.10.** Results of the addition of different amounts of TEOA.

TEOA (ml)	H <sub>2</sub> (μmol)
0.1	33
0.3	39
0.5	49.5
1	138

### Proposed mechanisms

In a photocatalytic system there are two interconnected processes. The first is the electron transfer cycle which was fully explained in Chapter 1 and the second is the catalytic cycle, which in this case involves the reduction of protons to H<sub>2</sub> as shown in Scheme 3.2. The most likely process for this will involve a metal hydride intermediate from reduction of a proton. These processes are represented in the proposed mechanism in Scheme 3.2. The first step is the reduction of the 18-electron starting dimer **A** to yield the mononuclear 17-electron species **B**. These electrons come from the electron transfer cycle. These species could interact with a proton to yield **C** or with a proton and additional electron to yield **D**. From this point the cycle could close by either a binuclear homolytic

reaction to produce H<sub>2</sub> or by a protonation of the Fe-H in a heterolytic pathway to produce H<sub>2</sub>.



**Scheme 3.3.** Proposed mechanism of catalytic cycle.

## Experimental

### Photocatalytic measurements:

In a typical photocatalytic experiment, a 20 ml glass vial with a magnetic stirrer bar was charged with 4ml of a solvent mixture, such as N,N-dimethylformamide (DMF), that contained the catalyst, the photosensitizer ([Ru(bpy)<sub>3</sub>](PF<sub>6</sub>)<sub>2</sub>), and the electron donor (e.g. triethanolamine (TEOA), trimethylamine (TEA) or 1-benzyl-1,4-dihydronicotinamide (BNAH)). The vial was then sealed and removed from the nitrogen filled glovebox. Vials were then subjected to irradiation from a set of LED lights with stirring for the desired time. (Figure 3.4)

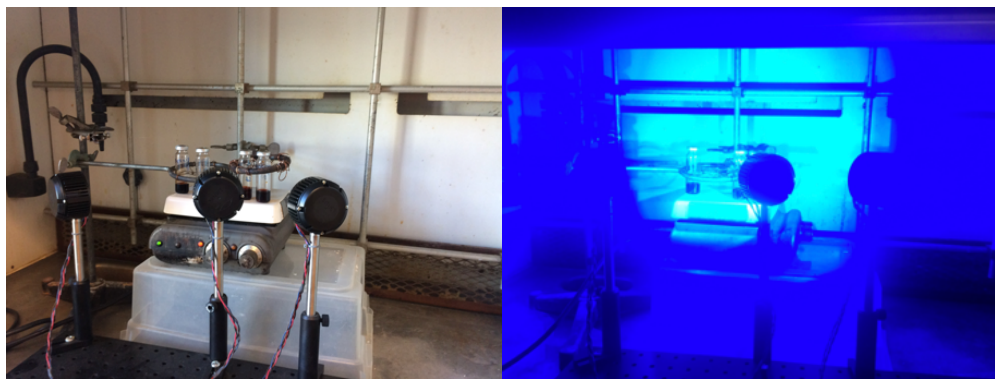


**Figure 3.4.** The photographs of the irradiation apparatus used for the photocatalytic experiments before and during the light irradiation.

### **Synthesis of 2,6-(CH<sub>3</sub>SCH<sub>2</sub>)<sub>2</sub>NC<sub>5</sub>H<sub>3</sub>**

The bis(methylthioether)pyridine ligand, 2,6-(CH<sub>3</sub>SCH<sub>2</sub>)<sub>2</sub>NC<sub>5</sub>H<sub>3</sub>, was synthesized, beginning with bis(chloromethyl)pyridine and NaSMe, according to published procedures.<sup>15</sup>

### **Synthesis of [M{κ<sup>3</sup>-2,6-(MeSCH<sub>2</sub>)<sub>2</sub>NC<sub>5</sub>H<sub>5</sub>}Br<sub>2</sub>]<sub>x</sub> (M= Mn, Fe, Co, Ni, Cu, Zn)**

Using a 1:1 stoichiometric ratio of ligand: MBr<sub>2</sub>, a direct, heterogeneous, room temperature reaction proceeded in toluene as indicated by color changes to the reaction mixture. Allowing the reactions to continue overnight provided optimal yields. The precipitation of the product solids was facilitated by cooling the reaction mixtures to -20°C and leaving overnight. The solids were then isolated by filtration and washed with hexanes to remove impurities. These reactions proceeded in near quantitative yields for the dibromides of Mn, Fe, Co and Zn, in an excellent, 84% yield in the case of Cu and a slightly lower yield of 64% for the Ni complex as summarized in Scheme 3.2.

MBr<sub>2</sub> powder (30 mg, 0.139 mmol) was added to a clear yellow solution of 2,6-(MeSCH<sub>2</sub>)<sub>2</sub>NC<sub>5</sub>H<sub>5</sub> (41.5 mg, 0.209 mmol) in 8 ml of toluene. The reaction mixture was allowed to stir for 14 hours. In case of the Iron complex, it gradually became opaque orange. The solution was cooled to -20°C overnight. A brown precipitate formed which

was isolated by filtration and washed with 5 x 2 ml hexanes and then dried under vacuum. A fine peach colored powder was isolated in 96% yield. Peach crystals suitable for X-ray analysis were grown by diffusion of hexanes into a saturated THF solution of 2 and storing at -20°C for several days.

### **Gas Analysis**

The gaseous products of reduction were measured using an Agilent 7820A gas chromatograph (GC) with an Agilent select permanent gases column and equipped with a thermal conductivity detector (TCD). Gas chromatography (GC) is a technique that is used to detect and quantify volatile compounds in the gas phase, and the thermal conductivity detector (TCD) is a commonly used for determining yields of gaseous product by integrating the area under the peak. In general, the chromatographic data is shown as a graph of detector response versus the retention time, and it gives a spectrum of peaks for the sample that will be injected to represent the substance analytes that are present in the sample eluting from the column at different times. Retention time can be used to identify analytes, and the area under a peak is proportional to the amount of the analyte present. The concentration of the analyte in the original sample can be determined by calculating the area of the peak using a calibration curve that can be created by determining the response for a series of concentrations of analyte. A calibration curve for hydrogen was prepared, and the amount of the hydrogen was determined using the integrated values for the hydrogen (5.393 min) and the calibration curve. (Figure3.4)

## Calibration Curve

Using the calibration curve and the 2 equations below, we were able to calculate the amount of H<sub>2</sub> in our 22ml vessel.

$$y = 64.462x - 211.93 \quad (1)$$

$$(x * 1000000 * 17) / (200 * 22400) \quad (2)$$

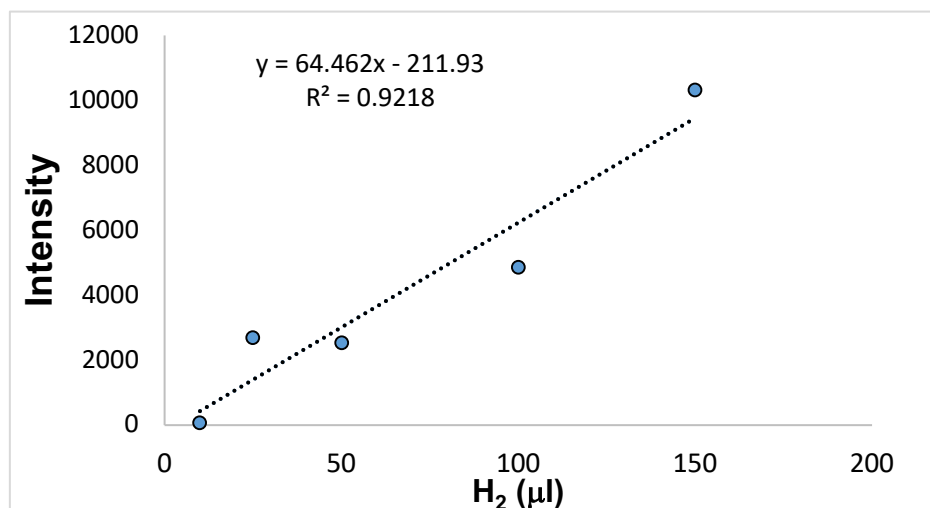


**Figure 3.5.** Calibration curve for calculation the amount of H<sub>2</sub> in the injected aliquot

Equation 1 gives us the amount of H<sub>2</sub> in μM from the injected amount which was 200 μM.

Then, using equation 2, we will be able to convert the x value taken by equation 1 into the whole amount of H<sub>2</sub> that we have in the 22 ml vessel.

These numbers are calculated by using a calibration curve taken from measurements by GC, there are two main errors, one from the calibration curve itself and the other is from the measurements of H<sub>2</sub>. Some of these errors were determined by multiple measurements of the same reaction by calculating the average of the products. To give the overall of the errors, the propagation of the errors from calibration curve and our own

results must be calculated. This calibration curve was obtained by other users and, as a result, we are not certain of the level of error in this data. This information could be combined with the errors of our GC measurements through propagation of error to provide a more definitive measure of the precision of our measurements.<sup>16</sup> Future investigators are encouraged to prepare a calibration curve with an error analysis so that such a treatment can be applied.

## **Conclusion**

Several first-row transition metal-based complexes with SNS ligand attached to them were synthesized and a preliminary study on their ability to reduce hydrogen using water as the hydrogen source showed that they were all capable of this reaction but with different activities. Among these, the iron complex,  $[\text{Fe}\{\kappa^3\text{-}2,6\text{-(MeSCH}_2\text{)}_2\text{NC}_5\text{H}_5\}\text{Br}_2\text{]}_2$  was chosen for further study. Results of blank experiments showed that the reaction was more productive without water which led us to better investigate the possible hydrogen source and we proposed that TEOA was acting as both ED and hydrogen source. Further studies on the catalyst stability proved that it was still productive after 72h.

## References

- 1 P. A. Chase, R. A. Gossage and G. Van Koten, *Modern organometallic multidentate ligand design strategies: The birth of the privileged 'pincer' ligand platform*, 2015.
- 2 E. Doomes, *J. Coord. Chem.*, 1976, **6**, 97–105.
- 3 P. Braunstein and F. Naud, *Angew. Chemie - Int. Ed.*, 2001, **40**, 680–699.
- 4 L. Canovese, F. Visentin, G. Chessa, P. Uguagliati, C. Levi and A. Dolmella, *Organometallics*, 2005, **24**, 5537–5548.
- 5 L. Soobramoney, M. D. Bala and H. B. Friedrich, *Dalt. Trans.*, 2014, **43**, 15968–15978.
- 6 M. Basauri-Molina, S. Hernández-Ortega and D. Morales-Morales, *Eur. J. Inorg. Chem.*, 2014, **2014**, 4619–4625.
- 7 H. Gamze, E. Aytar, M. Ulusoy, S. Demir and N. Dege, *Inorg. Chim. Acta*, 2018, **471**, 290–296.
- 8 Y. Hameed, S. Ouanounou, T. Jurca, B. Gabidullin, I. Korobkov and D. Richeson, *Polyhedron*, 2018, **154**, 252–258.
- 9 K. Kirchner, *Angew. Chemie Int. Ed.*, 2015, **54**, 4706–4707.
- 10 Y. Hameed, 2019.
- 11 H. Takeda, Y. Monma, H. Sugiyama, H. Uekusa and O. Ishitani, *Front. Chem.*, 2019, **7**, 1–12.
- 12 C. K. Prier, D. A. Rankic and D. W. C. MacMillan, *Chem. Rev.*, 2013, **113**, 5322–5363.

- 13 M. Taniguchi and J. S. Lindsey, *Photochem. Photobiol.*, 2018, **94**, 290–327.
- 14 A. Rosas-Hernández, C. Steinlechner, H. Junge and M. Beller, *Green Chem.*, 2017, **19**, 2356–2360.
- 15 L. Canovese, G. Chessa, G. Marangoni, B. Pitteri, P. Uguagliati and F. Visentin, *Inorganica Chim. Acta*, 1991, **186**, 79–86.
- 16 K. Arras and K. Arras, *Lausanne Swiss Fed. Inst. Technol. Lausanne*, 1998, 98–01.

## Chapter 4

### General Thesis Conclusions

This thesis presented a set of studies that were designed to interrogate two important aspects of the chemistry of hydrogen. One of these studies focused on unconventional catalysts for transfer hydrogenation of ketones to produce alcohols. The second was a search for a catalyst system that performs photocatalytic hydrogen production.

Understanding the background, context and literature precedent on these topics was presented in chapter one. In addition, common terms that are used and mechanisms which are proposed, were discussed.

In Chapter 2 the research goal was to develop a new transition metal complex for catalytic transfer hydrogenation of ketones to their alcohols. Considering sustainability, an iron complex was chosen as a starting point. As part of the optimization of the reaction parameters and background measurements the surprising discovery that the Fe complex was not necessary and that effective catalysis was achieved using the simple base, KO<sup>t</sup>Bu in catalytic amounts was obtained. In order to explore the generality of these results, several bases were examined and compared. In the case of the KO<sup>t</sup>Bu catalyst, the reaction parameters of temperature, time and catalyst loading were monitored. Results from works done by two different groups on catalytic reactivity of NaO did not align with neither us nor each other and they also claimed that KO<sup>t</sup>Bu was by far less reactive as a catalyst for this reaction, which possibly is as a result of different conditions. Therefore, we decided to do a thorough study on the catalytic TH potential KO<sup>t</sup>Bu.

Chapter 3 presented an exploration on the use of bis(thioether) pyridyl complexes of the first-row transition metals as photocatalysts for production of hydrogen using water as the hydrogen source. A scan of six complexes (M = Mn-Zn) indicated excellent activity of the Fe complex and this species was chosen for additional investigation. A more careful examination of the reaction conditions revealed the surprising result that this Fe complex was more effective in the absence of water. These studies have led to the proposal that the oxidized electron donor (e.g. TEOA or TEA) was the source of the observed hydrogen. A study has claimed that they were able to reduce hydrogen from water using Fe polypyridyl complexes but they never done a blank reaction to make sure about their argument.

Our success with both of these studies was gratifying and revealed the importance of careful control and background experiments when multicomponent, integrated systems are used. In both cases, the first and perhaps most obvious analysis was later revealed to be incorrect and in one case an alternative catalyst was active while in the other and unconventional substrate was the source of product.